High Energy Electron–Proton Physics at HERA

Report to the UK PPARC
Particle Physics Experiments Selection Panel

May 2000

H1 COLLABORATION PROPOSAL 750

The Universities of Birmingham, Lancaster, Liverpool, and Manchester, Queen Mary and Westfield College, University of London, and Rutherford Appleton Laboratory

with

RWTH Aachen (I and III Inst.), Universities of Brussels, Antwerpen, Cracow, Dortmund, JINR Dubna, CEA Saclay, DSM/DAPNIA, DESY–Hamburg, DESY–Zeuthen, Universities of Hamburg (II Inst.), Heidelberg, MPI Heidelberg, Universities of Kiel, Kosice, Lund, CPPM-Marseille, ITEP Moscow, LPI Moscow, MPI Munich, LAL Orsay, Ecole Polytechnique, Universities of Paris VI, Paris VII, Prague, Rome, PSI-Villigen, University of Wuppertal, Yerevan Physics Institute, ETH Zürich and University of Zürich

1 Introduction and Overview

In August 1998 the HERA electron-proton collider began to provide luminosity again after a long shutdown to enable the accelerator group and individual experiments to carry out maintenance and upgrade work. The proton beam energy was increased from 820 to 920 GeV and, for the first time since 1993, electrons were collided instead of positrons. A total of $9\,\mathrm{pb}^{-1}$ were delivered in 1998.

In 1998 several flagship measurements were made by H1-UK groups on the e^+p dataset of $35\,\mathrm{pb}^{-1}$ taken up to the end of 1997.

HERA continued to improve it's performance during 1999. Between January and April, $14.2\,\mathrm{pb}^{-1}$ of e^-p data were collected. A shutdown of two months then took place for further maintenance and upgrade work on all experiments and the collider itself.

From July to December, the accelerator ran successfully in e^+p mode, and H1 collected $20.9\,\mathrm{pb}^{-1}$ of data. A further sample of $4.6\,\mathrm{pb}^{-1}$ was taken with minimum bias triggers for precision measurements in the low parton-x region.

During 2000 the machine has continued to perform excellently in e^+p mode. In total, to date (02/05/00), H1 currently has accumulated $12.8\,\mathrm{pb}^{-1}$ of e^-p and $82\,\mathrm{pb}^{-1}$ of e^+p data. HERA will continue to run in e^+p mode until the next shutdown, with a final sample of over $100\,\mathrm{pb}^{-1}$ of data expected.

The large integrated luminosities will allow the experiment to carry out its full planned programme prior to the major upgrade of the HERA collider [1], to take place from September 2000. There will then be a shutdown of nine months, during which focusing magnets will be inserted in and around H1. The HERA upgrade is expected to yield a factor of five increase in luminosity delivered. Several components of H1 will be upgraded at the same time.

The UK groups have been heavily involved in many H1 activities in the past two years, making leading contributions to detector operation, physics analysis and upgrade preparations. Sections 2, 3 and 4 of this report contain short descriptions of these activities. Sections 7, 8, 9, and 10 document the publications, conference and workshop contributions and Ph.D. theses that have been produced as a result. For example, although contributing only 14% of the total physicist manpower on H1, members of H1–UK provide 1/3 of all H1 working group convenors. Furthermore, since our last report to the PPESP, our physics analyses have grown to include all areas of high P_T jet and lepton physics, whilst extending our expertise in low-x physics.

2 Physics Results

There have been a number of notable new results from the experiment in 1998 and 1999, with a strong UK involvement in many cases. A summary of analysis work from the past two years involving UK physicists is given below.

2.1 Deep–Inelastic Scattering at Very High Q^2

Inclusive Deep-Inelastic Scattering (DIS) cross-sections have long been used as sensitive probes of proton structure and QCD dynamics. The large integrated luminosity collected with both lepton charges in the colliding ep beams of the HERA accelerator have allowed the phase space of such measurements to be extended into new kinematic regions of very high Q^2, up to 30 000 GeV^2. In this region where $Q^2 \simeq M_Z^2$ or M_W^2, the Z^0 and $W^\pm$ boson masses squared, the electroweak sector of the Standard Model (SM) can be tested in DIS. In addition, signals of new physics beyond the Standard Model may be expected to arise at the highest Q^2 where the smallest distance scales of proton structure are probed.

The neutral current (NC) cross-section for the process $e^\pm p \to e^\pm X$ with unpolarised beams is given by

$$\frac{\mathrm{d}^2\sigma^\pm_{NC}}{\mathrm{d}x\,\mathrm{d}Q^2} = \frac{2\pi\alpha^2}{xQ^4}\left[Y_+\tilde{F}_2 \mp Y_- x\tilde{F}_3 - y^2\tilde{F}_L\right] , \tag{1}$$

where α is the fine structure constant and the helicity dependences of the electroweak interactions are contained in the functions $Y_\pm \equiv 1 \pm (1-y)^2$. The dominant contribution to the cross-section comes from the structure function $\tilde{F}_2$. The $\tilde{F}_L$contribution is largest at high y and is expected to diminish with increasing Q^2, whereas the structure function $x\tilde{F}_3$ contributes in the high Q^2 regime where the effects of Z^0 exchange are significant. Note that for unpolarized beams, $\tilde{F}_2$ is the same for electron and for positron scattering, while the $x\tilde{F}_3$ contribution changes sign as can be seen in eq. 1. For simplicity it is convenient to present the NC "reduced cross-section" $\tilde{\sigma}_{NC}(x,Q^2) \equiv \frac{1}{Y_+}\frac{Q^4\ x}{2\pi\alpha^2}\frac{\mathrm{d}^2\sigma_{NC}}{\mathrm{d}x\mathrm{d}Q^2}$.

The leading order double differential charged current (CC) cross-section for $e^-p \to \nu X$ may be written

$$\frac{\mathrm{d}^2\sigma^-_{CC}}{\mathrm{d}x\,\mathrm{d}Q^2} = \frac{G_F^2}{2\pi x}\left(\frac{M_W^2}{M_W^2+Q^2}\right)^2 x\left[(u+c)+(1-y)^2(\bar{d}+\bar{s})\right] , \tag{2}$$

where G_F is the Fermi coupling constant, and u, c, $\bar{d}$, $\bar{s}$ are the quark distributions in the proton. The cross-section for $e^+p \to \bar{\nu}X$ is obtained by exchanging all quarks with anti-quarks (and vice-versa) in eq. 2. The CC reduced cross-section is defined as $\tilde{\sigma}_{CC}(x,Q^2) \equiv \frac{2\pi x}{G_F^2}\left(\frac{M_W^2+Q^2}{M_W^2}\right)^2\frac{\mathrm{d}^2\sigma_{CC}}{\mathrm{d}x\mathrm{d}Q^2}$.

The single differential cross-sections $d\sigma/dQ^2$ for NC and CC DIS are shown in fig.1 for $y \leq 0.9$. The measurements show the now published e^+p data [2], and new preliminary measurements made using the e^-p data [3]. The positron data were taken at $\sqrt{s} \approx 300$ GeV, whilst the electron data were taken at $\sqrt{s} \approx 320$ GeV. The data are compared to the NLO QCD fit performed on low Q^2 fixed target data from NMC and BCDMS and H1 e^+p data, termed the "H1 e^+p QCD fit" in the following. The e^-p NC and CC measurements presented here were not included in the QCD fit.

The data are generally found to be in good agreement with the expectation, though an excess of approximately two standard deviations remains at the highest Q^2 in the NC e^+p data. For $Q^2 > 3\,000$ GeV^2 the NC e^-p cross-section is observed to be systematically larger than the e^+p cross-section. The influence of the increased centre-of-mass energy is indicated by the dashed line. It causes an increase in the cross-section of $\approx 7\%$ for $Q^2 < 1\,000$ GeV^2 rising to 50% at $Q^2 = 30\,000$ GeV^2. However, at high Q^2 this is approximately an order of magnitude smaller than the increase expected from the different lepton charge. The differences between the e^-p and e^+p cross sections are consistent with the SM expectation for the parity violating contribution of Z^0 exchange.

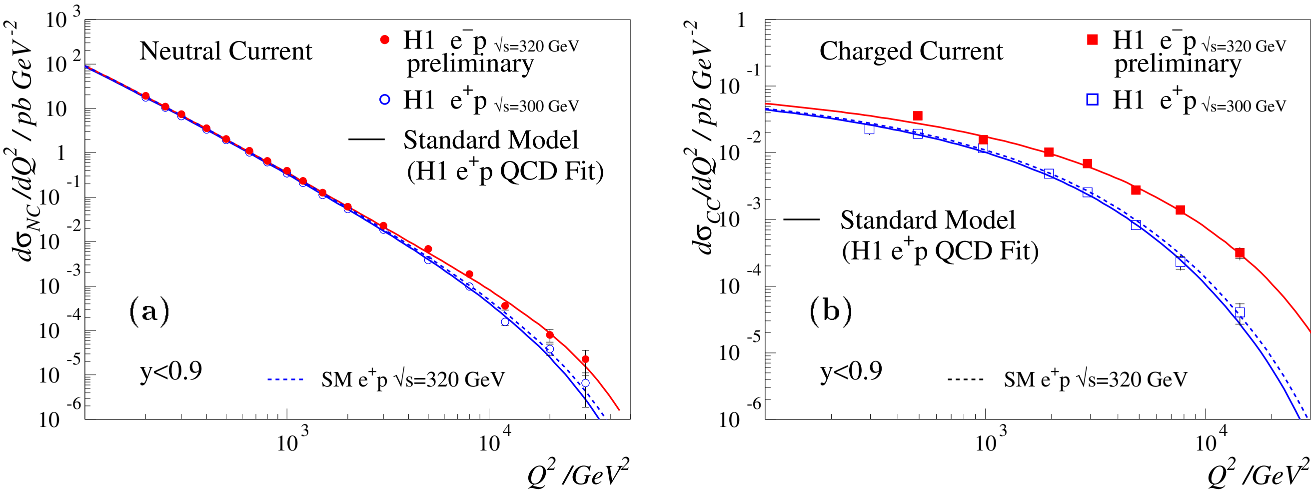

Figure 1: The Q^2 dependences of the NC (a) and CC (b) cross-sections $d\sigma/dQ^2$ are shown for the preliminary e^-p (solid points) and published e^+p (open points) measurements. The data are compared to the SM expectation. The influence of the increased centre-of-mass energy is shown as the dashed curve.

The Q^2 dependence of the CC cross-section for e^+p and e^-p scattering is shown in fig.1b. The electron data are found to have a larger cross section everywhere, by up to a factor of ten at $Q^2 = 15\,000$GeV^2. The effect of the increased centre-of-mass energy is expected to be relatively small, and is shown as the dashed curve in fig.1b. The CC cross-sections are in good agreement with the SM expectation based on the H1 e^+p QCD fit. The Q^2 dependence of the cross-section at high Q^2 is largely due to the effect of the electroweak propagator and is therefore sensitive to M_W. Fitting the e^+p data for the propagator mass yields the value $M_W = 80.9 \pm 3.3\,(\text{stat.}) \pm 1.7\,(\text{syst.}) \pm 3.7\,(\text{theo.})$ GeV. The theoretical uncertainty (theo.) is evaluated by varying the input assumptions and the data entering the fit. At the present level of precision, there is no evidence for any anomalous behavior and the value of M_W extracted is in agreement with time-like determinations [4]. Thus the results are consistent with the expected electroweak structure of the standard model in this newly probed deeply space-like region.

The double differential NC reduced cross-sections for e^+p and e^-p are shown in fig.2(a) which extends up to $x = 0.65$ and $Q^2 = 30\,000$ GeV^2. The data are compared to the H1 e^+p QCD fit, which is found to give a good prediction of the x, Q^2 behavior of the data. The two data-sets differ in the manner expected from parity violating contributions. These differences will allow a determination of the x$\tilde{F}_3$ structure function at high Q^2.

The double differential CC reduced cross-sections from electron and positron scattering are shown in fig.2(b). The data are well described by the H1 e^+p QCD fit. The cross-sections measured in e^-p scattering are found to be consistently larger than for e^+p scattering. The difference in the cross-sections is found to increase with Q^2. This is expected within the Standard Model and is due to the different quark densities probed in e^+p and e^-p scattering. Thus the CC cross-section is a powerful tool in refining our understanding of the flavour composition of the proton. With increased statistics, these are likely to become the definitive measurements. All of the H1 very high Q^2 data will improve considerably in both statistical precision and coverage of kinematic phase space as higher luminosity becomes available following the HERA upgrade.

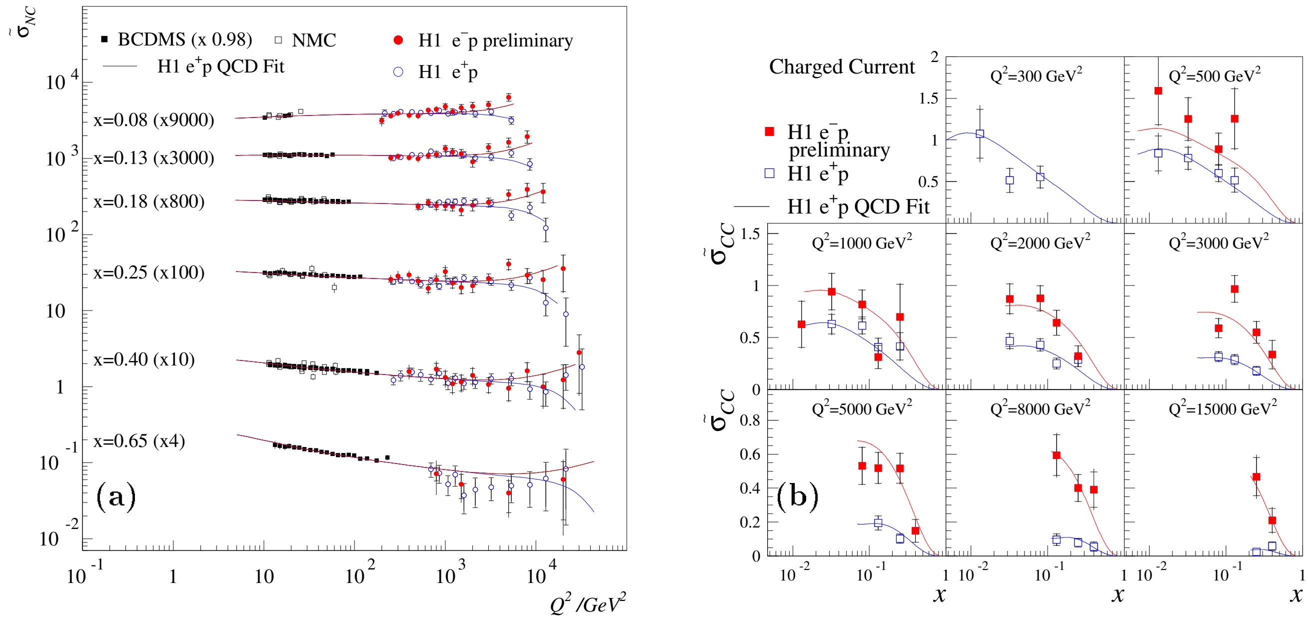

Figure 2: **(a)**The NC reduced cross-section $\tilde{\sigma}_{NC}$ is shown at high x for the preliminary e^-p data ($\sqrt{s} \approx 300$ GeV, solid points) and the e^+p data ($\sqrt{s} \approx 320$ GeV, open points) compared to the SM expectation. **(b)**The CC reduced cross-section $\tilde{\sigma}_{CC}$ is shown for the preliminary e^-p data ($\sqrt{s} \approx 300$ GeV, solid points) and the e^+p data ($\sqrt{s} \approx 320$ GeV, open points) compared to the SM expectation.

2.2 W Production

In the Standard Model W bosons are produced at HERA predominantly in photoproduction via bremsstrahlung off a quark ($ep \to eWX$). In certain scenarios beyond the Standard Model Ws may be produced via decays of heavier particles. For instance if single top quarks were produced (e.g. via the reaction $\gamma c \to t$, as proposed in [5]) Ws would be observed in the decay $t \to bW$. A similar decay chain occurs in supersymmetric models where the stop decays to W sbottom ($\tilde{t} \to \tilde{b}W$) [6]. In such models the W would be produced alongside a hadronic jet with high transverse momentum.

At H1 W events are identified in the $W \to e\nu$ and $W \to \mu\nu$ decay channels, by selecting events with large missing transverse energy and an isolated electron or muon [7, 8].

P_T^X >25 GeV

Data period	Data	SM
94-97 e^+p $(36.5pb^{-1})$	5	1.06±0.26
98-99 e^-p $(12.6pb^{-1})$	0	0.49±0.11
99-00 e^+p $(24.9pb^{-1})$	3	1.11±0.28
$\Sigma\ e^+$	8	2.17±0.52
$\Sigma\ e^+ + e^-$	8	2.66±0.60

Table 1: Observed and predicted event rates in the electron and muon decay channels combined, for each of the $\boldsymbol{ep}$ data periods 1994-2000. Also shown are the sum totals for all $\boldsymbol{e^+p}$ data, and for all $\boldsymbol{ep}$ data (H1 Preliminary).

A search was carried out using 12.8 pb^{-1} of e^-p scattering data and 61.3 pb^{-1} of e^+p scattering data.

A total of thirteen W candidate events were found, all of which appeared in the e^+p data sample. Five of these events were observed in the $W \to e\nu$ channel, compared to 5.89 ± 1.32 expected from Standard Model processes. The other eight candidate events were observed in the $W \to \mu\nu$ channel, compared to 1.96 ± 0.52 expected from Standard Model processes. In the e^-p data sample, no events were observed, which should be compared with 2.0 ± 0.4 events expected from Standard Model processes.

The events in both leptonic decay channels are particularly striking when studied as a function of P_T^X, the transverse momentum of the hadronic jet. At low P_T^X there is no significant deviation from the Standard Model. However, combining the electron and muon channels, 8 events were observed in the e^+p data sample, with $P_T^X > 25$ GeV, compared to 2.17 ± 0.52 events expected from Standard Model processes. A summary of the events observed in the three run periods can be found in table 1). Although the present number of candidate W events is small, the event yield after the HERA luminosity upgrade will increase by at least a factor of 10. Thus if the observed excess really is a signal of new physics such a discovery would certainly be made at HERA in the following years.

2.3 Diffractive Hard Scattering

The UK has traditionally been at the forefront of the H1 investigation into diffractive phenomena. This remains a fast developing field, with significant developments in the perturbative QCD (pQCD) description of hard diffraction in recent years. It is widely believed that an understanding of diffraction is the most important step necessary for a complete description of low-x physics.

The generic diffractive process at HERA is shown in figure 4. Experimentally, diffractive events in which the proton dominantly remains intact ($Y = p$ in figure 4) are characterised by large regions of the detector in the outgoing proton direction for which there is no activity, a 'rapidity gap'. The cross section for the process $\gamma^* p \to Xp$, where the photon dissociative system X is separated from the proton by a large rapidity gap, has been measured by H1 in the form of a diffractive structure function $F_2^{D(3)}(x_{\mathbb{P}}, Q^2, x/x_{\mathbb{P}})$ [11], where $x_{\mathbb{P}}$ is the fractional energy loss of the proton.

The diffractive structure function has been used to test diffractive factorisation hypotheses. The hard component of the diffractive DIS scattering amplitude has recently been shown to be factorisable [15], just as in standard DIS. Factorisation can be taken further under the assumption, inspired by Regge phenomenology, that there is a universal flux of an object with vacuum quantum numbers (the pomeron) associated with the proton [16]. Under this assumption, the parton distributions of the pomeron have been extracted from H1 F_2^D data at relatively low Q^2 [10].

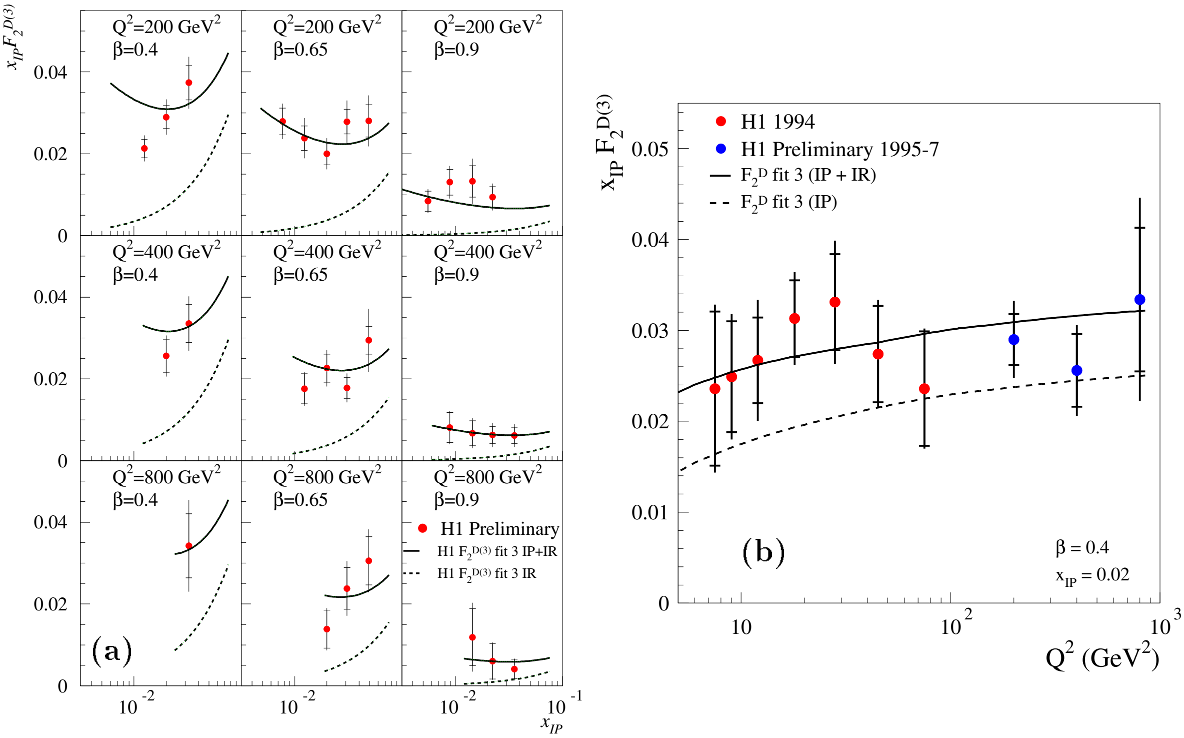

Figure 3: (a) The diffractive structure function at large Q^2, shown as a function of $x_{\mathbb{P}}$ in bins of fixed β and Q^2, compared to the extrapolation of a model based on DGLAP fits to lower Q^2 data, in which the pomeron structure is dominated by gluons carrying large fractional momenta. Both pomeron ($\mathbb{P}$) and sub-leading exchange ($\mathbb{R}$) contributions are included. (b) The Q^2 dependence of the diffractive structure function at example fixed values of β and $x_{\mathbb{P}}$, compared to the same model.

A new measurement [9] of $F_2^{D(3)}$ for $Q^2 \leq 800$ GeV^2, using data taken in 1995-7, is shown in figure 3a. It is compared with predictions based on the pomeron parton distributions extracted from the previous measurement [10], extrapolated to large Q^2 using the DGLAP evolution equations. The prediction with the leading pomeron and a sub-leading exchange included is in good agreement with the data. Figure 3b shows the Q^2 dependence of $x_{\mathbb{P}} F_2^D$ at a fixed value of $x_{\mathbb{P}}$ and $\beta = 0.4$. The rise in the structure function with Q^2 at such a large value of β lends support to the hypothesis that the pomeron is dominated by gluons carrying large fractional momenta.

A major activity at HERA over the past years has been the testing of the validity of these parton distributions for the description of as many diffractive observables at HERA as possible. The dijet and charm measurements described in the following sections provide perhaps the most stringent tests yet. They are both directly sensitive to the diffractive gluon distribution, which can only be inferred from scaling violations in more inclusive analyses.

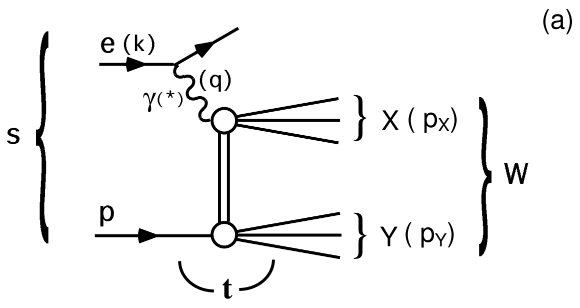

Figure 4: The generic diffractive process at HERA

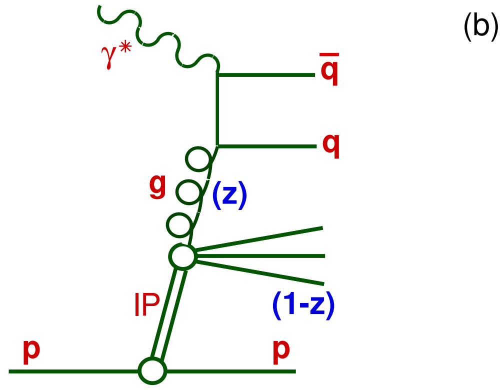

Figure 5: The dominant leading order QCD process for diffractive dijet and charm production in the partonic pomeron model.

2.3.1 Diffractive Dijet Electroproduction

Under the Regge factorisation ansatz, with the proton remaining intact, figure 5 represents the dominant dijet producing process at leading order of QCD. A gluon from the pomeron undergoes boson-gluon fusion with the virtual photon, such that the outgoing q and $\bar{q}$ may have high transverse momentum. The variable $z_{I\!P}$ then represents the fraction of the pomeron momentum that enters the hard scatter. A hadron level estimator of this quantity, $z_{I\!P}^{jets}$, is defined as

$$z_{I\!P}^{jets} = \frac{M_{12}^2 + Q^2}{M_X^2 + Q^2} \tag{3}$$

where M_{12} and M_X are the invariant masses of the dijet system and the full system X respectively.

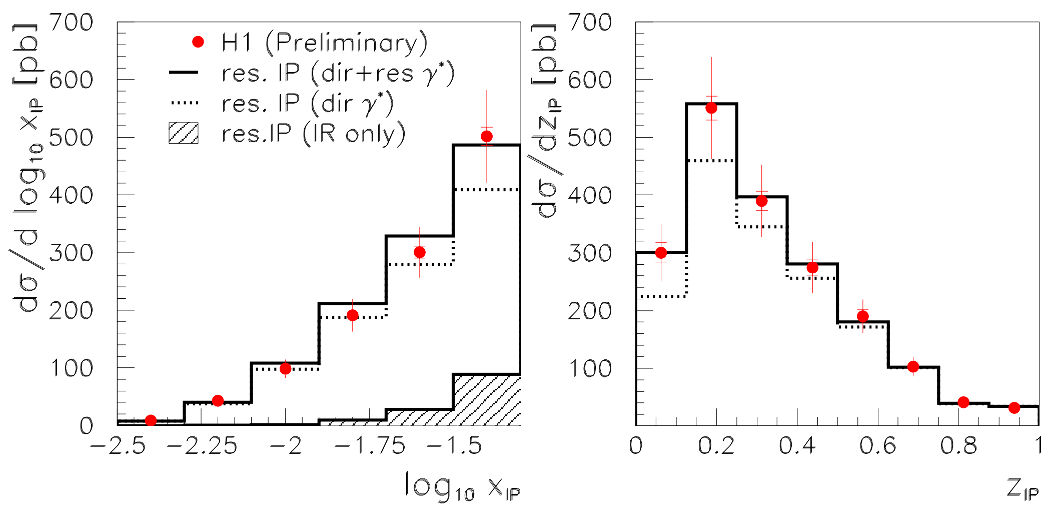

Figure 6: Differential hadron level cross sections for diffractive dijet production as a function of $x_{I\!P}$ and $z_{I\!P}^{jets}$. The data are for $4 < Q^2 < 80$ GeV^2 and the jets have transverse momentum $p_t^{jets} > 4$ GeV. The data points are compared with predictions based on pomeron and meson parton distributions extracted from $F_2^{D(3)}$, with a contribution in which the hadronic structure of the virtual photon is resolved.

The kinematic region probed in this analysis is determined to a large extent by the requirement that there be at least 2 jets with $p_t^{jets} > 4$ GeV in the X system. This forces $x_{I\!P}$ to be relatively large, and $z_{\mathbb{P}}$ typically to be small. Indeed, the fractional momenta accessed extend to values lower than those reached in inclusive analyses. Figure 6 [18] shows the corrected $x_{\mathbb{P}}$ and $z_{\mathbb{P}}^{jets}$ distributions compared, via a Monte Carlo model, with predictions based on pomeron and meson parton distributions extracted by H1 from analysis of $F_2^{D(3)}$ [11]. Since $p_t^{jets\ 2} > Q^2$ for much of the data, interactions involving resolved virtual photons are also included in the model. The agreement in both normalisation and shape between the factorisable pomeron model and the data is remarkably good, particularly since the kinematic ranges, experimental method and systematics are very different in the two cases. According to the models, approximately 75% of the dijet cross section can be attributed to hard scattering processes involving gluons from the pomeron.

2.3.2 Diffractive Dijet Photoproduction

Diffractive dijet measurements have also been made in the photoproduction ($Q^2 \to 0$) limit [21]. Figure 7 shows the data as a function of a hadron level estimator x_γ^{jets} of the fraction of the photon momentum entering the hard scatter. In photoproduction, there are clear contributions from resolved as well as direct photon interactions. Compared through the POMPYT Monte Carlo model with a prediction based on gluon dominated parton distributions extracted from F_2^D, reasonable agreement is again observed.

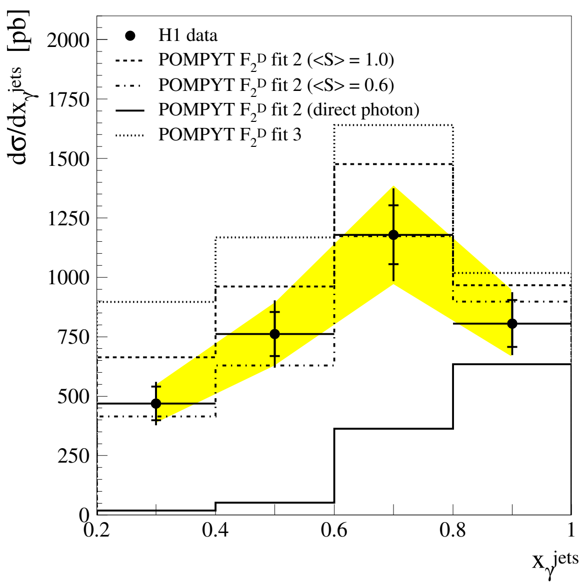

Figure 7: Differential cross section for diffractive dijet photoproduction as a function of x_γ^{jets}. The data are compared with the predictions of the POMPYT Monte Carlo model, based on two sets of gluon dominated pomeron parton distributions. The effect of possible rapidity gap destruction due to spectator interactions in resolved photon interactions is shown by applying a constant weighting factor $\langle S \rangle = 0.6$ to all resolved photon interactions in the simulation.

When the pomeron parton distributions from HERA are used to predict cross sections at the Tevatron, factorisation seems to be badly broken, with HERA based predictions failing by factors of up to 100 [17]. The most likely explanation is that where there are beam remnants on both sides of the rapidity gap, spectator interactions destroy the rapidity gap [22]. Such effects would always be expected in $p\bar{p}$ interactions, but in ep scattering, they would only be present in resolved photon interactions. It is very interesting that the region of figure 7 dominated by resolved photon interactions ($x_\gamma^{jets} \lesssim 0.8$) shows some evidence for an excess in the prediction.

Since both direct and resolved photon interactions are present, these data are likely to be very useful in the development of a phenomenological understanding of the failure of factorisation at the Tevatron, which has become a major challenge in low x physics.

2.3.3 Diffractive Electroproduction of $D^{*\pm}$ Mesons

Within the resolved pomeron model, the production of open charm occurs via the same mechanism as the dijets (figure 5), where the quarks emerging from the boson-gluon fusion process are a $c\bar{c}$ pair. The process has also been modelled using a pQCD approach to the pomeron structure based on 2-gluon exchange [19].

An analysis [20] has been performed using data collected during 1995, 1996 and 1997, corresponding to an integrated luminosity of 20.8pb $-$ 1. The D^{*+} mesons are reconstructed using the decay channel

$$D^{*+} \to D^0 \pi^+_{slow} \to (K^- \pi^+) \pi^+_{slow} \tag{4}$$

and its charge conjugate. The cross section in the kinematic range $2 < Q^2 < 100$ GeV^2, $0.05 < y < 0.7$, $x_{I\!P} < 0.04$, $M_Y < 1.6$ GeV, $|t| < 1$ GeV^2, $p_T(D^{*\pm}) > 2$ GeV and $|\eta(D^{*\pm})| < 1.5$ is

$$\sigma(ep \to (D^{*\pm} XY) = 154 \pm 40(stat.) \pm 35(syst.)\text{pb}. \tag{5}$$

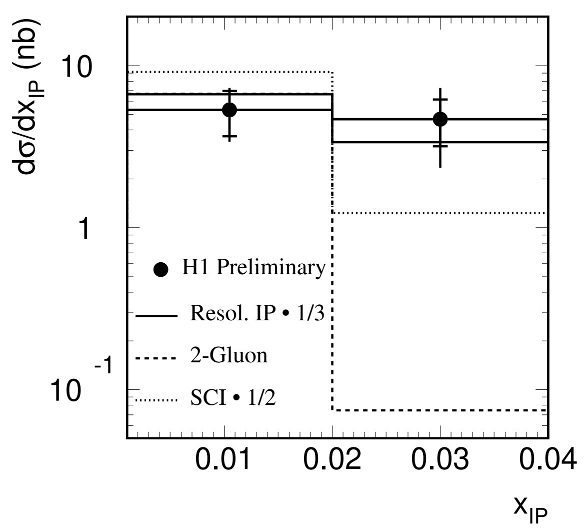

Figure 8: The cross section $\sigma(ep \to D^{*\pm}XY)$ measured differentially in $x_{I\!P}$.

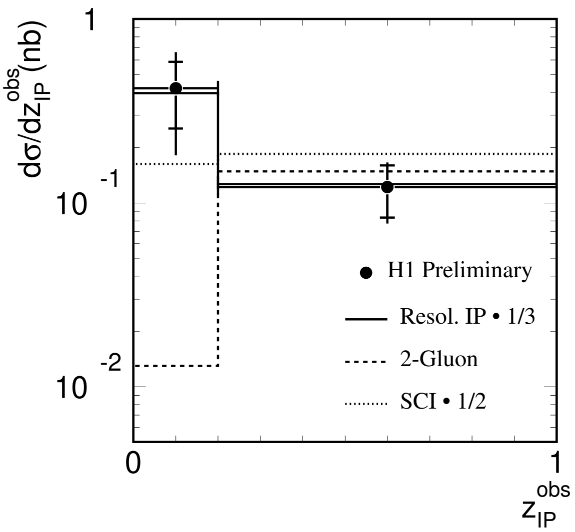

Figure 9: The cross section $\sigma(ep \to D^{*\pm}XY)$ measured differentially in $z^{obs}_{I\!P}$.

The cross section is shown differentially as a function of $z^{obs}_{I\!P}$ and $x_{I\!P}$ in figures 8 and 9. In the present version of the two gluon exchange model, only the case in which the parton level final state system X consists of a $c\bar{c}$ pair is implemented. In the regions where the X system must have this basic parton level configuration (high $z^{obs}_{I\!P}$ and low $x_{I\!P}$), the model successfully predicts the magnitude of the cross section. However, the two gluon model fails in the regions of higher mass for the system X, i.e. low $z^{obs}_{I\!P}$ and high $x_{I\!P}$. Calculations where $c\bar{c}g$ final states are also considered are likely to improve the description in these regions.

The partonic pomeron model predicts the shape of all the differential distributions well (further distributions can be found in [20]). The overall normalisation fails by a factor of 3, however. This effect may be the first indication of a failure of the partonic pomeron model in DIS. The large increases in statistics that are likely to be available after the upgrade will help resolve this question.

2.3.4 Diffractive Scattering at Large Momentum Transfer

Events with large rapidity gaps in the hadronic final state and a perturbatively hard scale at one end of the exchange have long been recognized as a unique place to study the interplay between long and short distance physics. Measurements of diffractive deep inelastic scattering at HERA [11], for example, have led to a phenomenology which mixes the languages of both perturbative QCD and Regge theory. A particularly special class of events in which there are hard scales at both ends of the exchange has also been observed at both the Tevatron [23, 24] and HERA [25], and is the subject of this study. Such events are characterised by two hard jets in the final state separated by a large rapidity interval and an absence of energy above some small scale between the jets. One might expect to be able to calculate the rate for such process using only perturbative methods, since the gap producing mechanism is squeezed to small distances [26]. This approach is dependent on the construction of a colour singlet object within perturbative QCD, a problem that is far from resolved. Calculations using the leading logarithmic approximation of BFKL [27] have been performed by Mueller and Tang [28] and found to describe the Tevatron gaps between jets data [29] and the related process of high-t vector meson production at HERA [30, 31]. The situation is complicated, however, by the issue of rapidity gap survival probability; interactions, which may be hard or soft, between spectator partons in the colliding hadrons can destroy the gap [32, 33]. This introduces a potentially large non-perturbative component into the calculation of gaps between jets, making absolute predictions of both rates and differential distributions problematic [29]. A purely perturbative prediction is possible if a dijet gap event is defined in terms of some minimum energy, $Q \gg \Lambda_{QCD}$, between the jets [34]. This measurement is designed specifically to allow such calculations to be compared to data.

The data for this analysis were collected with the H1 detector during the 1996 running period, when HERA collided 27.6 GeV positrons with 820 GeV protons, with an integrated luminosity of 6.2 pb^{-1}. Photoproduction events were selected by detecting the scattered positron in the electron tagger of the luminosity system. This restricts the virtuality of the photon to $Q^2 < 0.01$ GeV^2. The photon-proton centre of mass energy is restricted to the range $165 < W < 233$ GeV to avoid regions of low electron tagger acceptance.

The inclusive k_t clustering algorithm [35] was applied to the hadronic final state objects. Objects are defined using a combination of tracking and calometric information which improves the resolution compared to methods using only single detector components. Events with 2 or more jets identified by the above algorithm were kept if the two highest E_t jets in the event satisfied the following criteria:

$$E_t^{jet1} > 6.0\,\mathrm{GeV} \tag{6}$$

$$E_t^{jet2} > 5.0\,\mathrm{GeV} \tag{7}$$

$$|\eta^{jet1}, \eta^{jet2}| < 2.8 \tag{8}$$

$$\Delta\eta > 2.5 \tag{9}$$

The total transverse energy between the jets, $\not{E}_t^{jets}$, is defined as the sum of the energy of all jets (hereafter referred to as minijets) between the axes of the two highest E_t jets, i.e.

$$\not{E}_t^{jets} = \sum E_t^{minijets} \;\; , \;\; \eta_{forward}^{jet} > \eta_{minijet} > \eta_{backward}^{jet} \tag{10}$$

A rapidity gap event is defined as an event in which $\not{E}_t^{jets} < E_t^{cut}$, where E_t^{cut} is varied between 0.5 GeV and 5.0 GeV. Such a definition has the advantage of being completely infra-red safe, and relatively insensitive to hadronisation effects. Details can be found in [36].

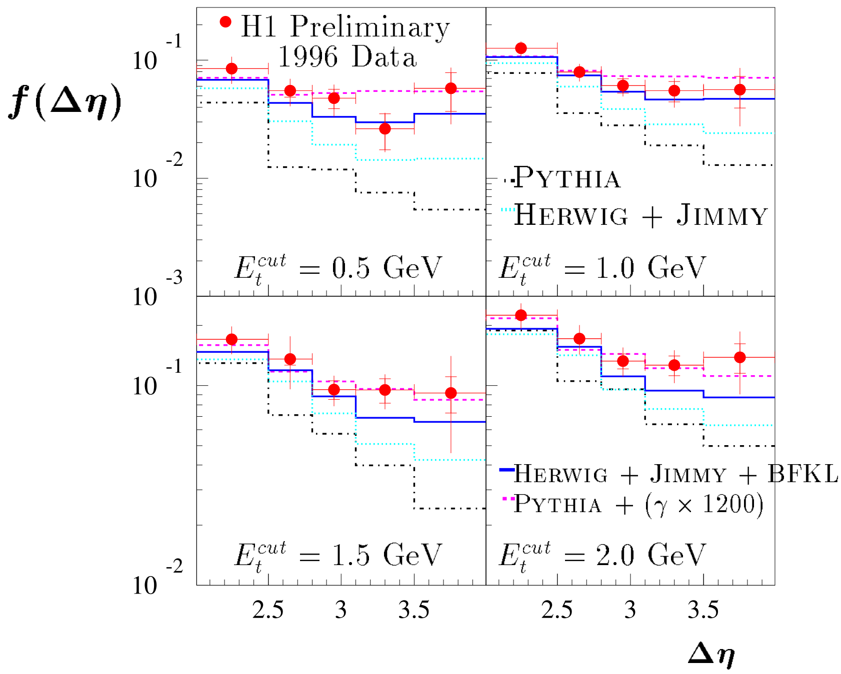

Figure 10: The gap fraction differential in $\Delta\eta$ for $E_t^{cut} = 0.5, 1.0, 1.5, 2.0$ GeV , compared to different Monte Carlo models. Herwig + BFKL is a HERWIG 5.9 + Jimmy photoproduction sample with BFKL colour singlet exchange added according to the generated cross section with $\alpha_s = 0.17$. PYTHIA + ($\gamma \times 1200$) is a PYTHIA photoproduction sample with high$-t$ photon exchange added, with the generated cross section multiplied by a factor of 1200. Also shown are HERWIG 5.9 + Jimmy and PYTHIA 5.7 photoproduction samples with no colour singlet component added.

The gap fraction, defined as the ratio of the gap and inclusive cross sections, is shown in figure 10 differentially in $\Delta\eta$. Also shown are the predictions of several Monte Carlo models.

PYTHIA clearly underestimates the observed gap fraction. With the addition of an (unphysically large) sample of high-t photon exchange events, PYTHIA is able to describe the gap fraction for all values of E_t^{cut}. Similarly the HERWIG with JIMMY sample is unable to describe the observed gap fraction, although the predicted gap fraction is significantly higher than that from PYTHIA . With the addition of the BFKL sample a good description is obtained. This is a significant observation, since the normalisation of the BFKL sample was not fitted to the data, but resulted from the reasonable choice of $\alpha_s = 0.17$ in the LLA BFKL calculation of Mueller and Tang [28]. Such a choice was also found to fit the Tevatron gaps between jets data [29], suggesting that the normalisation of the BFKL pomeron cross section is relatively insensitive to the scale at which the hard scatter takes place.

2.4 Diffractive Vector Meson Production

The elastic and quasi-elastic production of vector mesons provide a useful testing ground for models of diffraction. While Regge theory with a soft pomeron describes photoproduction of light vector mesons well, processes where either Q^2 or the meson mass is larger show a steeper energy dependence [12,13,38]. In perturbative QCD (pQCD), which is expected to be valid for sufficiently large Q^2 or mass, this behaviour is driven by the increase in the gluon density of the proton as x decreases.

2.4.1 Elastic J/ψ Electroproduction

Figure 11 shows photon-proton cross sections for elastic J/ψ production, $\gamma^* p \to J/\psi\, p$, as a

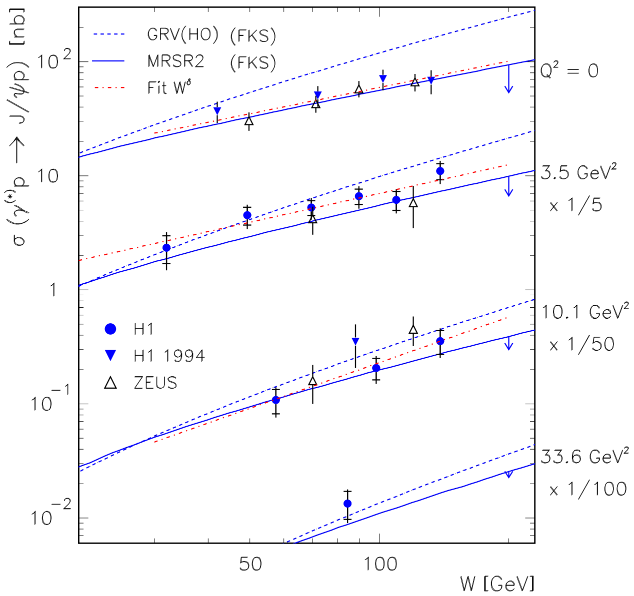

Figure 11: Cross sections for elastic J/ψ production as a function of W at different values of Q^2, measured at HERA. The cross section at $\langle W \rangle = 32\,\mathrm{GeV}$ and $Q^2 = 3.5\,\mathrm{GeV}^2$ was measured using events in which one of the muons from the decay $J/\psi \to \mu^+\mu^-$ was detected in the FMD.

function of the centre-of-mass energy W for several values of the photon virtuality Q^2. The data can be described by QCD models (e.g. [14], labelled 'FKS' in the figure) based on the exchange of gluon pairs from the proton. The results [13] use data from 1995 to 1997 to provide more precise measurements in a larger kinematic range then earlier analyses. The Forward Muon Detector (FMD) has been used to extend the coverage to lower energy, $\langle W \rangle = 32.0\,\mathrm{GeV}$, at $Q^2 = 3.5\,\mathrm{GeV}^2$. This has the advantage of narrowing the gap in energy between the other results from HERA and those from fixed-target experiments, and enables an investigation of the energy dependence which is independent of other experiments. To measure this data point, events were used in which one muon from the decay $J/\psi \to \mu^+\mu^-$ was reconstructed in the FMD while the other was identified using the Liquid Argon Calorimeter or the Central Muon Detector. A sample of events with both muons in the FMD was used as a check on the detector efficiency. Mass spectra for both samples are shown in figure 12.

2.4.2 Elastic J/ψ and Υ Photoproduction.

Measurements have recently been published of an analysis of elastic J/ψ and Υ photoproduction [37]. The strong rise of the elastic J/ψ photoproduction cross section reported at the Tampere Conference is confirmed [38]. The data are now of sufficient precision to allow the W dependence to be investigated in several regions of t, the four-momentum transferred from the virtual photon to the proton, as shown in figure 13. The rapid increase with W is observed to occur in each t range.

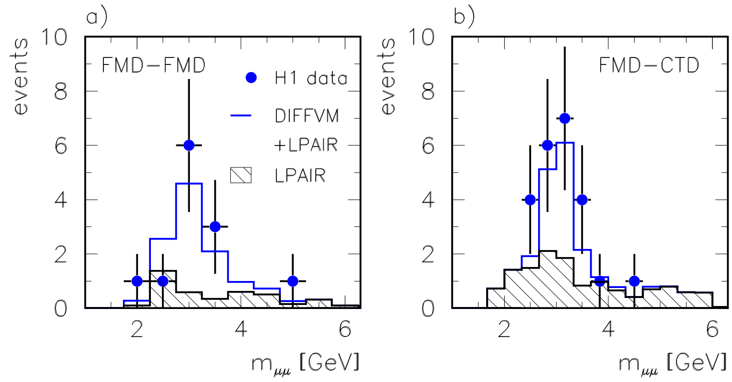

Figure 12: Mass spectra from events in the low-W J/ψ sample. (a) Events with both muons in the FMD. (b) Events with one muon in the FMD and the other in the central region, used in the published measurement. The uncorrected data are compared with the sum of a diffractive J/ψ production model (DIFFVM) and a contribution (LPAIR) from the background process $\gamma\gamma \to \mu^+\mu^-$.

In perturbative QCD the production mechanism is thought to be mediated by the exchange of two gluons so that the cross section is proportional to the square of the gluon density of the proton [39]. The rapid rise of the gluon density as Bjorken x decreases is then responsible for the observed sharp rise of the cross section with W. The observed cross section for Υ is also compatible with the predictions of a model based on this approach [40].

Non-perturbative models of the production mechanism have been developed which involve pomeron exchange. Figure 13 shows that the standard soft pomeron exchange [41] gives too slow a rise with W to be compatible with the data. However, an extension of such models [42] invoking the exchange of a further hard pomeron allows a satisfactory description of the data. A model for the pomeron based on a NLO BFKL calculation [43] is also compatible with the data. The fits to the data in figure 13 have been used to search for shrinkage of the diffraction peak. The constant slope of the increase with W in the different t ranges is compatible within large errors with little shrinkage. These fits allow, for the first time, the extraction of the effective Regge trajectory exchanged in J/ψ photoproduction from a single experiment avoiding the relative normalisation uncertainties due to systematic effects between the experiments.

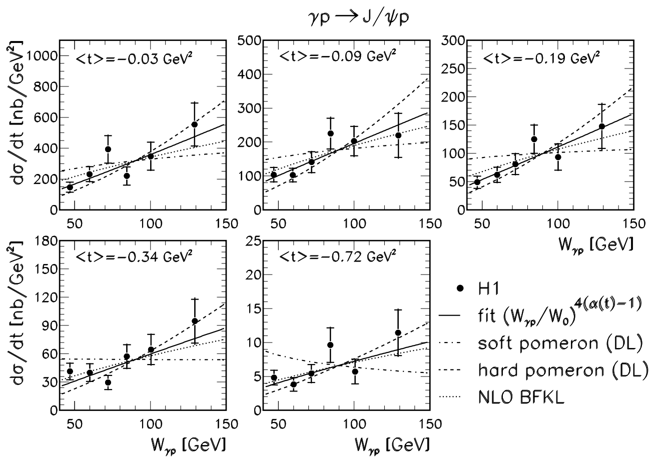

Figure 13: The differential cross section as a function of W together with the fit of the Regge trajectory (solid line). The predictions of the soft and hard pomeron trajectories [42] are shown as the dash-dotted and dashed lines. The prediction based on a NLO BFKL calculation [43] is given as the dotted line.

2.5 The Hadronic Final State at HERA

The hadronic final state from ep collisions offers a rich testing ground for testing the theory of Quantum Chromodynamics (QCD). High transverse momentum jet and particle production directly probe pQCD processes and reveal the partonic structure of the proton and photon. Hadron properties at low momentum are sensitive to the hadronisation process and can thus be used to assess the environmental dependence of fragmentation and test non-perturbative QCD models of hadron production.

Since the last report, members of the H1-UK community have maintained their involvement in this field and have played leading roles in the following works.

2.5.1 High P_T Forward Particle Production at low x

A study of particle production in the region near to the fragmenting proton (the forward region) was recently made to resolve one of the open questions at HERA: how do partons evolve from the proton? Parton evolution based on the DGLAP equations successfully describes all inclusive measurements of the proton structure function F_2. However, this scheme sums terms in $\ln(Q^2)$ and ignores terms in $\ln(1/x)$ which should play a significant role in the low x domain opened by HERA and therefore BFKL evolution which, conversely, sums terms in $\ln(1/x)$ should become important. The BFKL and DGLAP equations prescribe different dynamical features of the

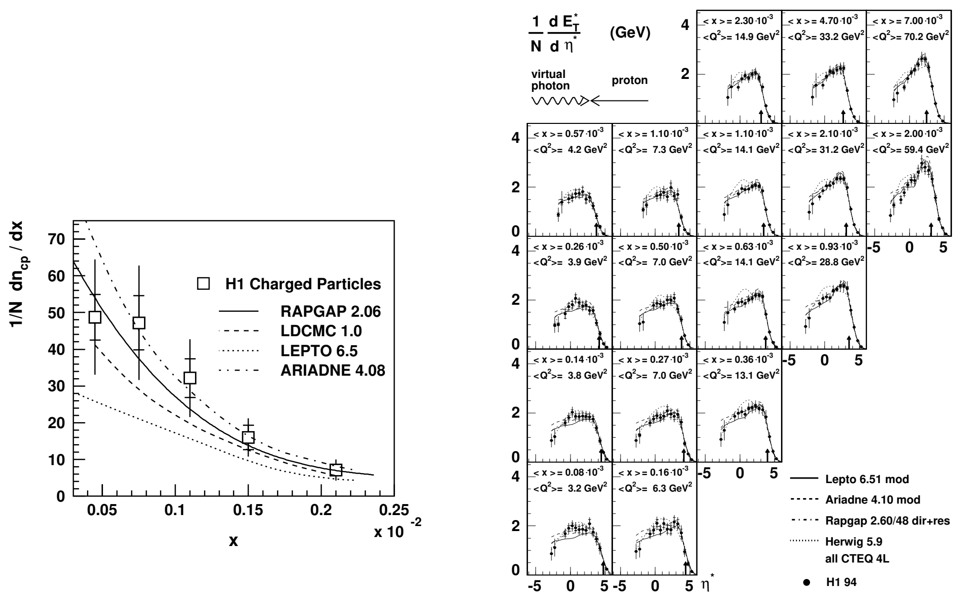

Figure 14: The x dependence of the rate of high transverse momentum forward charged particles inclusively produced in DIS interactions (left). The inclusive transverse energy flow $1/NdE_T^*/d\eta^*$ at different values of x and Q^2 (right). The predictions of QCD-based models are also shown.

evolving partons with BFKL evolution expected to give rise to more high transverse momentum emissions. Thus a measurement of the rate of high transverse momentum particle production in the region associated with the parton evolution was made [44]. The rate of particles inclusively produced in the forward region with transverse momentum of greater than 1.0 GeV is shown in figure 14 (left) as a function of x and rises as x decreases. Predictions from several QCD-based models are also shown. Calculations which only implement DGLAP evolution from the proton produce insufficient QCD radiation in the forward region to match the data at the lowest values of x.

2.5.2 Transverse Energy Flow

In addition to the charged particle studies, the UK groups been active in making measurements of transverse energy [45]. These contain global information about charged and neutral particles and cover a wider pseudorapidity range than equivalent charged track studies.

Figure 14 (right) shows the inclusive transverse energy flow $1/NdE_T^*/d\eta^*$ in DIS interactions as a function of pseudorapidity (η^*) in the photon-proton centre of mass system in different regions of x and Q^2, for a range in pseudorapidity which extends over 8 units. As x and Q^2 increase the energy flow shows a clear peak in the region associated with the fragmentation of the struck parton indicating that hadrons are increasingly collimated. QCD-based calculations which implement different approaches to produce higher order QCD emissions are tested by the data.

2.5.3 Strange Particle Production

The flavour structure of the hadronic final state contains information about the partonic composition of the proton and sheds light on the hadronisation process. The H1 collaboration has recently made the first measurements of charged kaon and pion production in the low x domain [46]. Figure 15 shows the differential transverse momentum spectra $\frac{1}{N}\frac{dn}{dp_T^{*2}}$ of charged kaons inclusively produced in DIS interactions. The rate reduces as the transverse momentum increases.

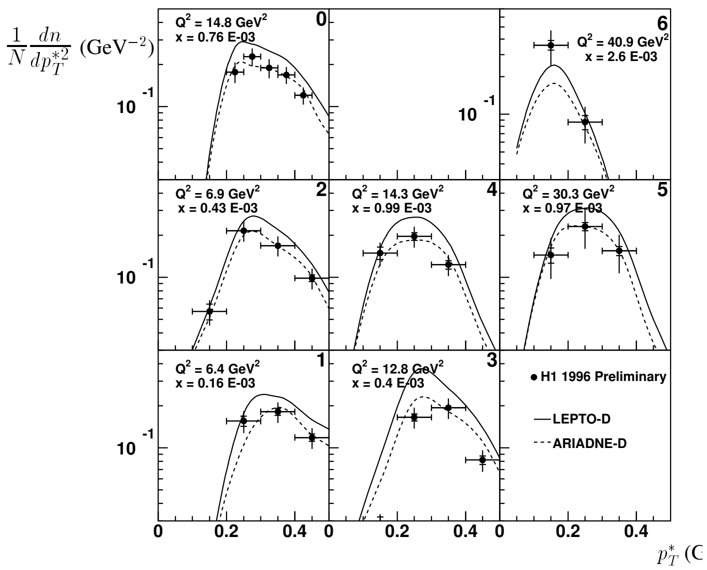

Figure 15: The inclusive charged kaon distributions $\frac{1}{N}\frac{dn}{dp_T^{*2}}$ in different intervals of x and Q^2. The predictions of QCD-based models are also shown.

There is no large dependence on the kinematics of the DIS interaction. QCD-based models which use a string fragmentation approach determined from e^+e^- data are compared with the data. These models describe the data well, thereby supporting the hypothesis of the environmental independence of hadronisation. The value of the 'suppression factor' in low x DIS, corresponding to the ratio of probabilities of vacuum production of $s\bar{s}$ pairs to the lighter $u\bar{u}$ and $d\bar{d}$ pairs, $\mathcal{P}(s\bar{s})/[\mathcal{P}(u\bar{u}) + \mathcal{P}(d\bar{d})]$ was found to be approximately 0.23.

2.6 QCD Studies in the Breit Frame at HERA

2.6.1 Introduction

Studies of DIS ep processes in the Breit frame of reference by the UK groups have recently been published [50–53]. These have included the energy behaviour of the moments of the fragmentation function, invariant energy spectra and the correlation between the charge of the hadronic final state and the charge of the scattered parton [54]. Some of these are described below.

2.6.2 Scaling Violations of the Fragmentation Function

In figure 16, the fragmentation function is plotted in intervals of the scaled momentum variable, x_p, as a function of the invariant four-momentum transfer, Q. The function shows a strong rise at small x_p with increasing energy which becomes flatter in the larger x_p region. Predictions based on NLO QCD calculations [55] (dotted line) have a tendency to overestimate the inclusive particle production cross section in the small x_p, low Q region where the available phase space for fragmentation is strongly suppressed.

These mass effects are neglected in the pQCD approach but may be taken into account by means of a "power-correction" factor of the form

$$F = \left(1 + \left(\frac{\mu}{p_h}\right)^2\right)^{-1}$$

Here, p_h is the momentum of the final state hadron and μ is a free parameter that sets the hadronic mass scale. The solid line in figure 16 shows the result of applying this correction ($\mu = 300$ MeV) to the NLO calculation. The agreement with the H1 ep data over the available phase space is remarkable.

2.6.3 Rapidity Distributions

Figure 17 presents the rapidity spectra [56] for high Q^2 data integrated over all transverse momenta, and binned in various p_t intervals. The proton remnant extends toward large positive rapidity. At low transverse momenta a clear plateau in the target hemisphere (the proton remnant extends toward large positive Y) can be seen. As the average p_T of the particles increase, QCD effects gradually evolve the flat plateau into an almost Gaussian structure peaking near the origin of the Breit frame axis ($Y = 0$).

Predictions based on Local Parton Hadron Duality indicate the appearance of two distinct plateaux with a 9/4 ratio in their respective heights reflecting the colour charge of the dominant gluonic radiation in the target hemisphere [57] as opposed to the exchange quark in the current region. Despite many tests to isolate events in which such behaviour might be expected to be amplified, we have been unable to observe a double plateaux structure.

In figure 18, the rapidity spectra are shown binned in two Q^2 intervals for charged tracks with transverse momenta above 1 GeV. At low Q^2 a peak is clearly seen in the target region, while at higher Q^2 the peak shifts in the direction of the current region.

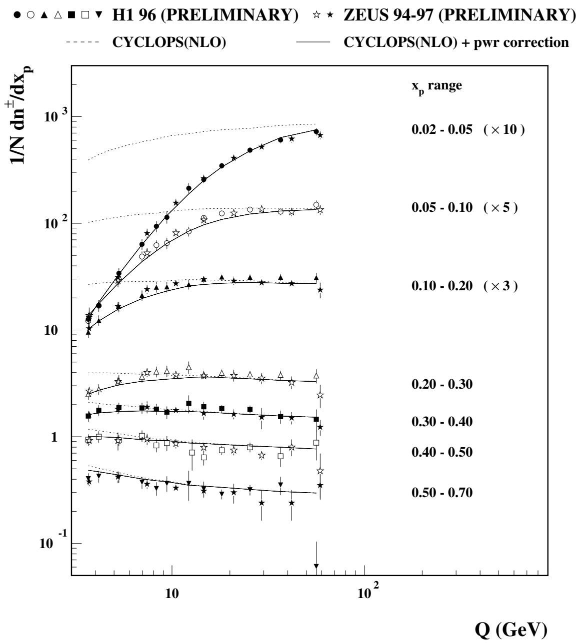

Figure 16: The fragmentation functions are plotted for different intervals of x_p as a function of Q^2 and compared with e^+e^- data at equivalent centre-of-mass energies, E^*. Note that the data for the three smallest intervals of x_p are scaled by factors of 10, 5 and 3 for clarity. The dotted and solid lines show the predictions of the CYCLOPS NLO with and without the power correction respectively.

In the naive QPM, the transverse momentum of the hadronic final state arising from the scattering of a massless parton ($m = 0$) is due largely to hadronisation effects and is small, typically much less than 1.0 GeV. However, if the scattered parton is off the mass-shell (mass $m >> 0$) then it may branch via gluon bremsstrahlung e.g, QCD Compton. Viewed in this frame, the topology of the event depends on the size of the quark-gluon invariant mass relative to the four-momentum transfer of the exchanged photon. For $m/Q \approx 1$ the quark-gluon system is at rest and back-to-back. Approximately half of the hadronic fragments related to the initial struck parton are scattered into the current hemisphere while the other half are scattered into the target hemisphere. For $m/Q >> 1$, both the quark and gluon are boosted forward into the target hemisphere giving a large observed p_T in this region. The current region is completely devoid of hadronic fragments (empty). For $m/Q << 1$, both the quark and gluon are boosted backward into the current region giving large p_T in this region. With increasing Q, events with $m/Q >> 1$ become less significant [58]. The mean transverse energy flow measured in the hadronic centre-of-mass system exhibits a similar shift with increasing photon virtuality [59].

2.7 Virtual Photon Structure at HERA

Studies of the structure of virtual photons using high transverse momentum (P_t) jets have now been extended to the case where there are two such jets in the final state. The photon, with virtuality Q^2, is probed with a resolution given by the P_t^2 of the jets. With dijet events it is possible to reconstruct x_γ, the fraction of the virtual photon's momentum carried by the parton participating in the hard scattering process. In leading order dijet production, $x_\gamma < 1$ for resolved photon processes and $x_\gamma = 1$ for direct. Because of the presence of two hard scales, Q^2 and P_t^2, and the point-like coupling at the core of the fluctuations leading to the partonic structure of the photon, virtual photon structure is quite unlike that of hadrons. As the

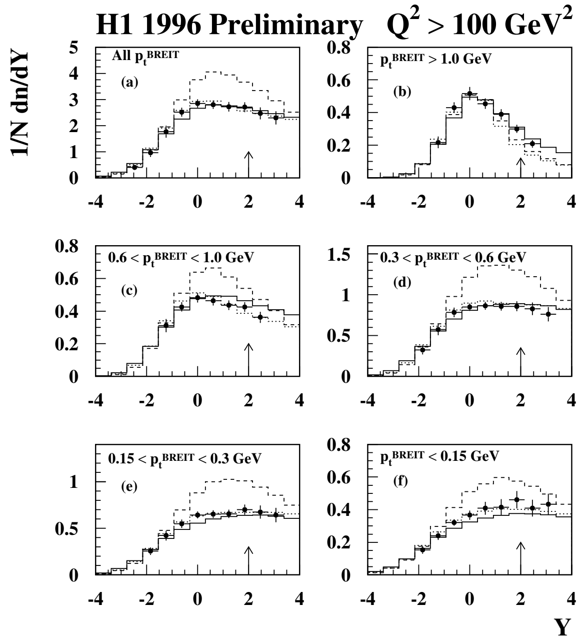

Figure 17: The rapidity distribution for (a) all charged tracks, and (b-f) for the five indicated intervals of track transverse momentum, p_t^{BREIT}, in the Breit frame, all at high Q^2. The error bars show the sum of statistical and systematic errors added in quadrature. The arrow indicates the position of the origin of the hadronic centre of mass system for the $\langle Q \rangle$ (23 GeV) of the data. The histograms show the predictions of LO Monte Carlo models, the solid line using a color dipole fragmentation, the dashed (dotted) lines utilising a parton shower model with(without) soft colour interaction effects.

probing scale increases, the probability of finding a parton at high x_γ increases. Furthermore, in addition to this unique scaling-violation behaviour, perturbative QCD is also able to predict the evolution of the photon structure with its virtuality in the region $P_t^2 \gg Q^2 \gg \Lambda^2$. Here, the target virtuality provides a natural cut-off, the leading log behaviour of the photon structure is $\sim \ln(P_t^2/Q^2)$ and so the virtual photon parton densities are slowly suppressed as $Q^2 \to P_t^2$. Away from this region, various models have been proposed to interpolate between the low- and high-Q^2 domains [48].

H1 have investigated the virtual photon structure as functions of x_γ, probing scale and target virtuality [49]. The triple-differential cross-section, $\mathrm{d}^3\sigma_{ep}/\mathrm{d}Q^2\mathrm{d}\overline{E_t}^2\mathrm{d}x_\gamma^{jets}$ ($\overline{E_t}^2$ is the mean E_t of the two highest E_t jets and x_γ^{jets} is the value of x_γ calculated from them), was determined and then this was used to measure, for the first time, an effective parton density (EPDF) of the virtual photon. The study spans the range $1.6 < Q^2 < 80\mathrm{GeV}^2$ with $0.1 < y < 0.7$, using data taken in 1996.

Both the triple-differential cross-section and the effective parton density show the characteristic behaviour predicted by models based on perturbative QCD. For example, the cross-section is shown in figure 19 as a function of x_γ^{jets} in ranges of Q^2 and $\overline{E_t}^2$. It decreases rapidly with increasing $\overline{E_t}^2$ and with increasing Q^2 in a manner consistent with the logarithmic suppression inherent in the models of virtual photon structure with which it is compared. The shaded histogram shows the expectation from a model with point-like coupling of photons only. This is clearly unable to describe the data except in the highest x_γ^{jets} bin and possibly also in the highest Q^2 range.

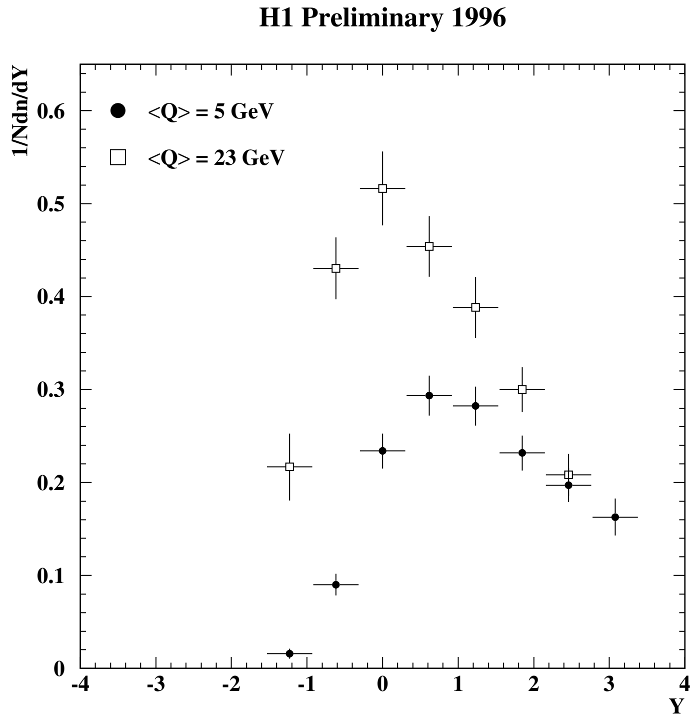

Figure 18: Preliminary 1996 rapidity distributions in the Breit frame of reference for two Q^2 intervals at high p_T. With increasing Q^2, the peak of the distribution is observed to shift from the target region to the current region of the Breit Frame. This shift is due to the interplay of QCD effects and kinematics.

2.8 Open Beauty Production

Due to the very small production cross sections, the study of beauty production at HERA has barely begun. The first measurement at HERA of open beauty photoproduction has recently been published [47]. The technique used was to select an enriched sample of semi-leptonic b decays on the basis of muons with a $p_T > 2$ GeV embedded within jets. The sample contained about 50% b events with 50% background with equal contributions from the semi-leptonic decay of charm and from light hadrons. These backgrounds were measured from the data and subtracted to obtain the beauty signal. The total leptoproduction and photoproduction cross sections were measured from the 1996 data. Figure 20 shows the result, which is somewhat above the value expected from the photon-gluon fusion process computed at Next-to-Leading Order of QCD. The higher luminosity data from 1997 and beyond are being used to check this result and measure the beauty production cross sections as a function of kinematic variables such as W and Q^2.

3 Detector Status and Developments

All the detector components described below remain the principal responsibility of UK groups. During HERA running periods each device requires more or less continuous attention from dedicated physicists, either directly at DESY or remotely from the UK via computer link.

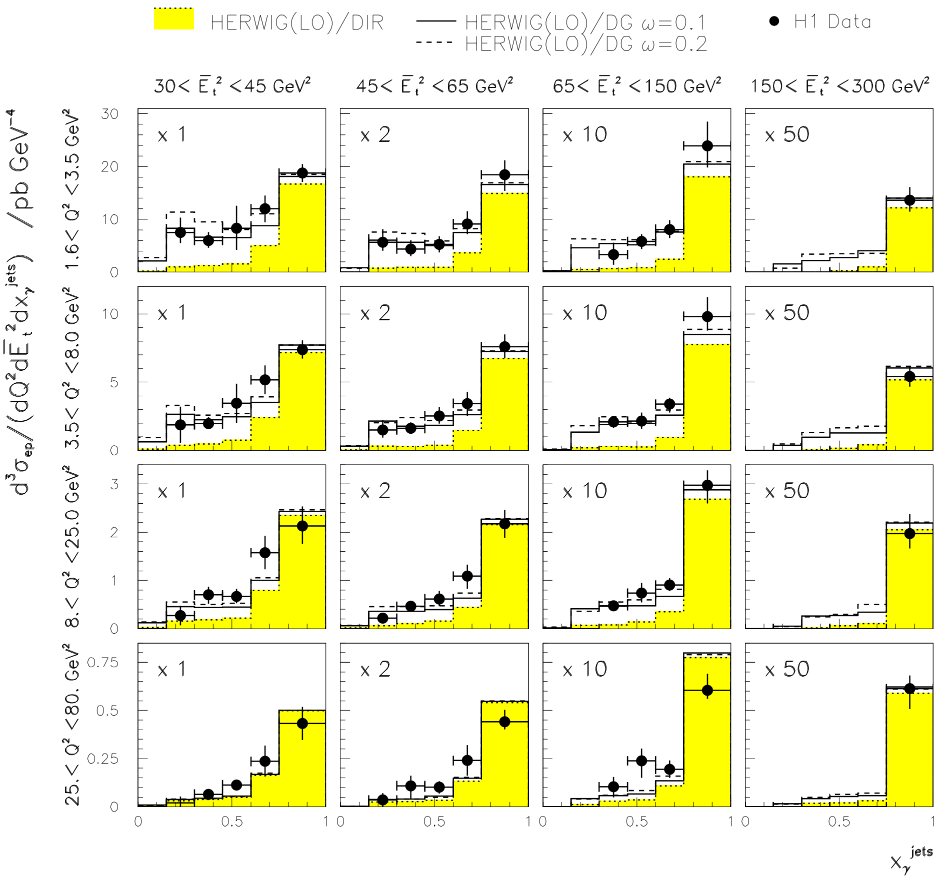

Figure 19: The differential dijet cross-section $\mathrm{d}^3\sigma_{ep}/\mathrm{d}Q^2\mathrm{d}\overline{E_t}^2\mathrm{d}x_\gamma^{jets}$ shown as a function of x_γ^{jets} for different regions of $\overline{E_t}^2$ and Q^2. Note the indicated scale factors applied to the cross-sections. The error bar shows the quadratic sum of systematic and statistical errors. The absence of a data point indicates that no measurement was made because of insufficient statistics for the two dimensional unfolding. The predictions of various models for virtual photon structure are also shown. The shaded histogram shows the prediction of a model which does not include virtual photon structure.

3.1 Data Acquisition and Silicon Tracker Readout

During 1998 and 999 the data acquisition and readout systems continued to operate and perform reliably. These systems, which are based on the VMEbus standard, have been described extensively in previous reports. Optical fibres are used to interconnect over 100 electronics crates containing the necessary ADCs and several hundred microprocessors. The introduction of the PCI standard has considerably enhanced the system potential which, together with Power PC technology, has resulted in more compact solutions performing at increased data throughput rates.

Preparations are now being made for the expansion of the RAL-designed Silicon Readout System to cater for more detector components, namely the Forward Silicon Tracker. This will result in nearly 3/4 million total silicon channels being read out by the system.

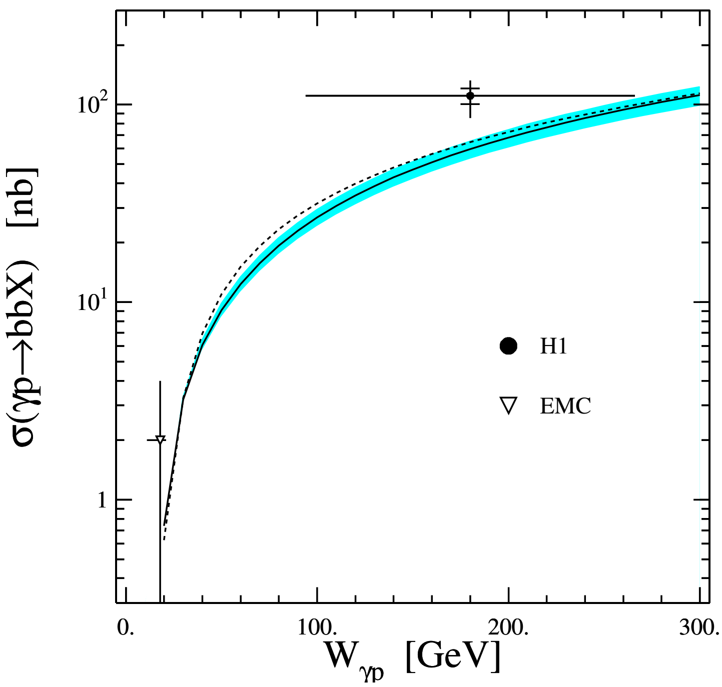

Figure 20: H1 and EMC results on the total photoproduction cross section for the process $\gamma p \to b\bar{b}X$. The curves represent NLO QCD calculations with varying choices for the parton distributions of the proton, the factorisation and renormalisation scales.

3.2 Backward Calorimeter Timing

The timing electronics and monitoring procedures for the SpaCal lead/scintillating fibre calorimeter have also continued to function reliably during 1999. No particular problems arose from the different operating conditions implied by the changes in lepton beam charge and proton beam energy. During the year QMW physicists provided on-call expert help and contributed to ongoing analysis work to improve trigger selectivity and calibration as well as to the publication of a summary paper [60] on this detector.

3.3 Forward Muon Detector and Trigger

The Forward Muon Detector (FMD) and Forward Muon Trigger have performed smoothly during 1998 and 1999, despite a couple of hardware problems. The system has been maintained by the Birmingham and Manchester groups. The currents drawn by the sense wires in the FMD drift chambers have increased in line with the increased beam currents injected by HERA. Hardware problems occurred with a mass flow meter responsible for determining the gas mixture and with a CAEN HV module; it emerged that the chambers had been damaged but, after a detailed study, it was concluded that the damage was not permanent. No effect on track reconstruction was observed, and since the effect was in a post-toroid layer, it did not interfere with the use of the pre-toroid layers as a veto for diffraction analyses.

In 1999 the H1 publication on charmonium production [13] in DIS included a cross section for low W elastic production of J/Psi measured using the FMD. A similar measurement for photoproduction is to be included in a forthcoming H1 paper.

3.4 Forward Track Detector

The Forward Track Detector (FTD) has performed well during most of 1998 and 1999 under the direct control of UK physicists resident at DESY, with monitoring and calibration in the hands of UK based scientists via remote computer link.

In October 1999 a serious leak occurred in the cooling system between the Central and Forward Track Detectors. In order to keep the temperature of the detector-mounted pre-amplifiers of both the FTD and the central tracker within safe limits, it proved necessary to run without power to the FTD Radial chambers. The resulting 7% loss in FTD track finding efficiency and 15% degradation in precision are unfortunate but unavoidable consequences of that safety requirement, which ensures that the electronic and structural components of the FTD chambers survive undamaged for the upgrade. Repair of the leak will take place during the next HERA shut-down.

3.5 Energy Scale Group

UK physicists lead the effort within H1 to obtain the best possible understanding of the calorimeter energy scales. In addition to an overall coordination rôle, UK physicists have completed calibration analyses which have dramatically improved the precision of measurements which rely on the LAr calorimeter. The overall scale uncertainty on hadrons measured in the LAr has been reduced from 4% to 2% (a factor 2 better than design). For the bulk of electrons measured in the LAr the uncertainty has been reduced from 2% to 0.7%. Furthermore, these analyses determine the correlation properties of the calibration such that the actual reduction in the final uncertainty for new analyses is greater than the naive expectation. For example, a reduction in the error for jet cross sections at high P_T^2 of a factor of up to 16 is possible.

4 Upgrade Projects

The UK groups are responsible for two major projects for the forthcoming upgrade, which will ensure that we exploit fully the increased luminosity after 2001.

4.1 Forward Track Detector Upgrade

There were significant developments in the programme to upgrade the H1 Forward Track Detector (FTD) [61] during 1999. Firstly, the design of the structure that will support the GO magnet that is to extend through the foremost two thirds of the FTD was completed; the support required will be mounted between the Central and Forward Track Detectors and can only be accommodated if the FTD is shortened somewhat. Secondly, as the operation of the Planars proved to be more stable than that of the Radials during high background electron-proton running, the decision was taken to remove not only the MWPCs and the Transition Radiators from the FTD, but also the Radials and use the space so created to insert not three new Planars, as originally planned, but five. The resulting upgraded FTD design is shown in figure 21. Note that the new Planars contain 8 sense wires as opposed to the 4 wires in the original chambers. This aids resolution of the left-right ambiguity and further improves the pattern recognition capabilities of the FTD. The design of the new Planars was completed early in 1999 and construction started at Daresbury once the necessary clean room space had been built. Three chambers have now been constructed and are under test. The Daresbury team can produce two chambers a month, allowing the comfortable completion of the chambers required for installation in H1 within the HERA upgrade schedule.

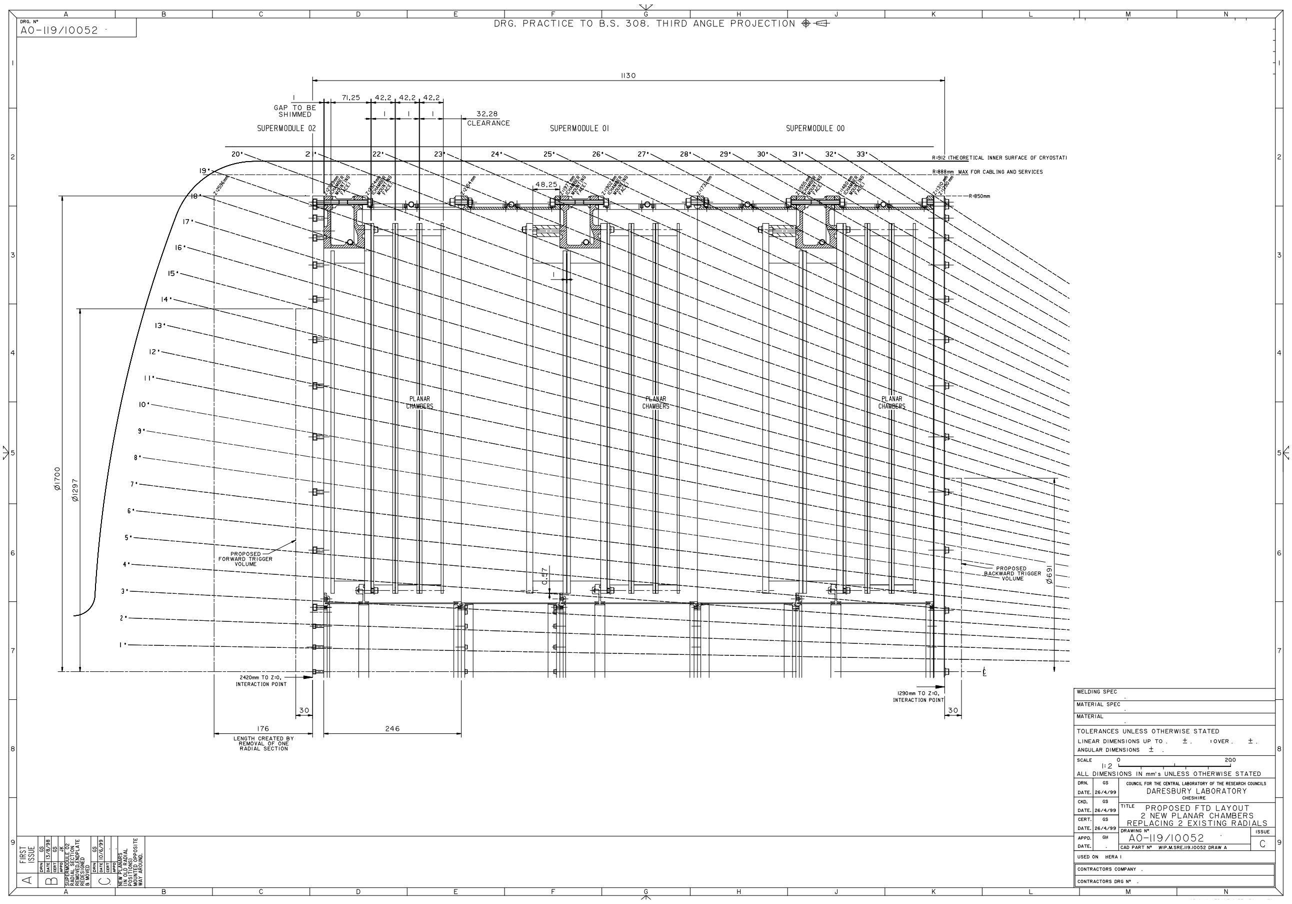

Figure 21: The plans for the Upgraded Forward Track Detector.

The software needed for the simulation, readout and calibration of the upgraded FTD is being developed in parallel with the construction of the new Planars, as is the necessary reconstruction code.

4.2 Track Trigger Upgrade

A high resolution Fast Track Trigger (FTT) [62] is being built for implementation in H1 after the luminosity upgrade in 2000 in order to extend the triggering capabilities for exclusive final states involving tracks. This is aimed at enhancing the trigger efficiency for exclusive physics in the absence of any high p_t particles, thus allowing precision measurements of rare processes such as D^* production using the high post-upgrade luminosity. The project represents one of the most ambitious attempts to reconstruct tracks with high precision down to low p_t in the real time environment necessary for triggering in high multiplicity events at a collider. Extremely good selectivity is achievable by combining the tracks to form invariant mass calculations.

The aim is to have track information from the Central Jet Chamber with which to make basic selections at the first level trigger (L1), full track based selections at level 2 and kinematic selection using combinations of tracks at level 3 (the latter in around 100 μs). The UK groups have undertaken the design and construction of the L1 part of this system. As illustrated in figure 22, this requires the digitisation of the analogue signals from the drift chamber, highly parallel "Q/t" analysis, local track segment finding in fast FPGA arrays and application of the L1 trigger logic, all within 2.3 μs of the interaction. The segment information is then distributed appropriately for the later track linking and fitting in the L2 system.

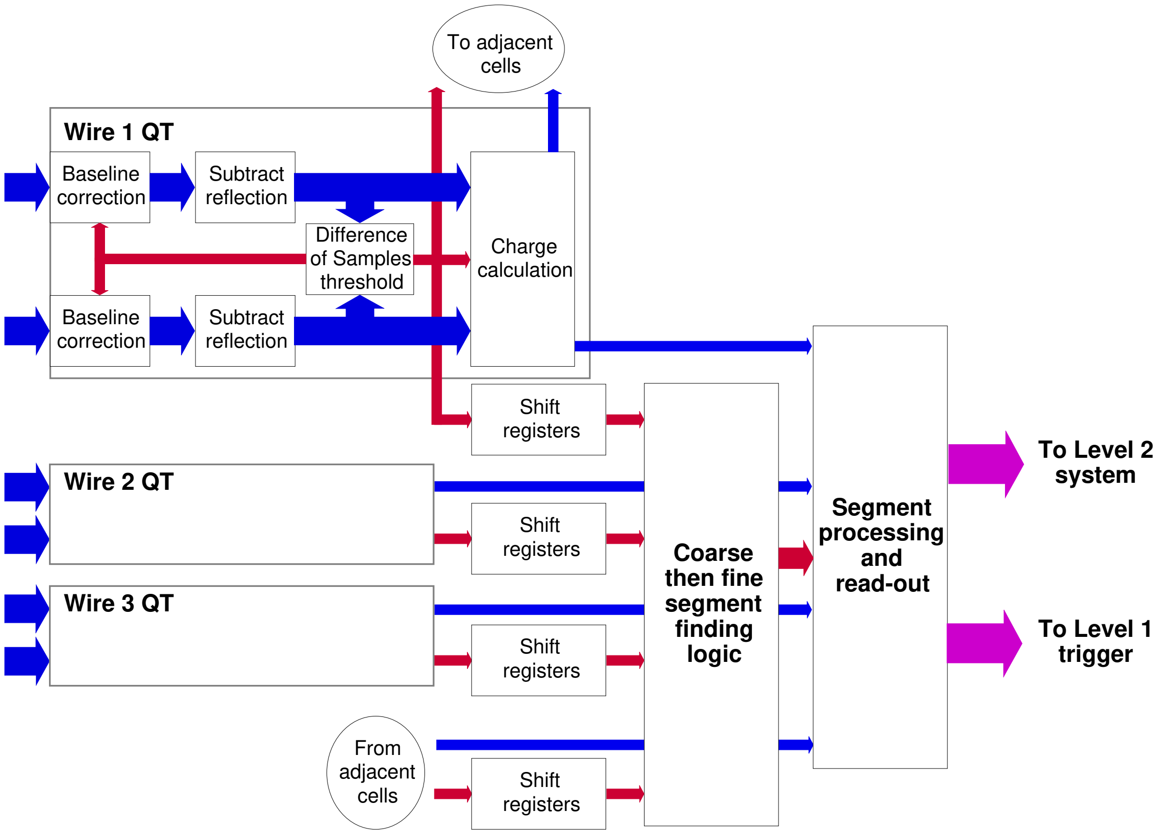

Figure 22: Block diagram of the Fast track Trigger algorithm for finding track segments from groups of three drift chamber wires.

5 Summary

The UK groups have continued to be prominent in all areas of H1 activity, taking leading roles in physics analysis, detector maintenence and upgrade projects. 1999 saw easily the largest volume of data collected in a single year to date. The analysis of this data is likely to yield many exciting results in the coming years. With the HERA upgrade due to commence in September 2000, still larger luminosities are soon to be expected. The future of the H1 experiment therefore looks bright for several years to come. The UK groups intend to continue to be at the forefront of this cutting edge experiment.

6 Future Plans and Requests to the PPESP

6.1 Continuation of the H1 Physics Program

Following the HERA upgrade, UK physicists will contine to play a leading role in the analysis of the data collected by H1. UK physicists are convenors of three of H1's seven physics working groups, namely the Flow and Spectra, High p_T/Q^2 and Jets groups. To give a few examples, our analysis plans for the period following the upgrade include the measurement of the CC and NC DIS cross–sections at high Q^2 for both electrons and positrons as a function of beam polarity, the extraction of the parton densities in the proton, the study of W production and decay in both leptonic and hadronic modes and the investigation of charm production at high x.

UK physicists currently lead two of the three technical working goups within H1 and will continue to do so following the upgrade. These are the Escale group, responsible for improving the understanding of the calibration of the H1 calorimeters, and the Fit group, which is examining the application of fitting techniques in a variety of contexts.

The UK will continue to be responsible for the Data Acquisition system and the Silicon DAQ, the Forward Muon Detector and its trigger electronics, the upgraded Forward Track Detector and the SpaCal timing electronics. To this come our new responsibility for the Fast Track Trigger.

6.2 Requests to the PPESP

As discussed in the above, the period following the HERA upgrade promises to be a fruitful one for H1. We, the UK groups within H1, have been prominent in preparing H1 for the luminosity upgrade and request continuation of PPARC support to allow us to reap the rewards of our preparatory work. We ask that the PPESP keep in mind that UK physicists have played and will continue to play a leading role in extracting physics from H1. This, coupled with our important new and continuing contributions to the H1 detector are likely to result in increased burdens in both Travel and Subsistence and Maintenance and Operation.

We request continued and adequate funding to support travel to Hamburg and to maintain and operate the detectors for which the groups are responsible. Both the FTD Upgrade and Fast Track Trigger projects will require extra travel in the short term and increased M&O commitment in the longer term, which changes are reflected in the following estimates shown in table 2.

Year	2000/1	2001/2	2002/3	2003/4	2004/5
M&O	50	60	75	75	75
Travel	310	310	290	290	290

Table 2: Requested funding in units of thousands of pounds sterling

We also request that the UK contribution to the H1 Common M&O fund be maintained at its present level of about 350kDM subject to the usual period dependent factors.

References

[1] 'The HERA Luminosity Upgrade', ed. U. Schneekloth, *DESY-HERA* **98-05** (1998).

[2] H1 Collaboration, *DESY* **99-107**, accepted by *Eur. Phys. J.*

[3] H1 Collab., 'Measurement of Neutral and Charged Current Cross-Sections in Electron-Proton Collisions at Large Momentum Transfer at HERA', paper 157b contributed to EPS99, Tampere, Finland, 1999.

[4] CDF Collaboration, F. Abe et al., *Phys. Rev. Lett.* **75** (1995) 11.
DØ Collaboration, B. Abbott et al., *Phys. Rev. Lett.* **80** (1998) 3008.
ALEPH Collaboration, R. Barate et al., *Phys. Lett.* **B422** (1998) 384.
DELPHI Collaboration, P. Abreu et al., *Eur. Phys. J.* **C2** (1998) 581.
L3 Collaboration, M. Acciarri et al., *Phys. Lett.* **B413** (1997) 176.
OPAL Collaboration, K. Ackerstaff et al., *Eur. Phys. J.* **C1** (1998) 395.

[5] H. Fritzsch, D. Holtmannspötter, *Phys. Lett.* **B457** (1999) 186.

[6] T. Kon, T. Matsushita, T. Kobayashi, *Mod. Phys. Lett.* **A12** (1997) 3143.

[7] H1 Collaboration, C. Adloff et al., *Eur. Phys. J.* **C5** (1998) 575.

[8] H1 Collaboration, 'W production in $e^{\pm}p$ collisions at HERA', Paper prepared for Lepton-Photon '99, Stanford, USA, 1999.

[9] H1 Collaboration, Conf. Paper 571, 29th Intern. Conf. on HEP, Vancouver, Canada (1998).

[10] H1 Collaboration, C. Adloff et al., Z. Phys. **C76** (1997) 613.

[11] H1 Collaboration, C. Adloff et al., *Z.Phys.* **C74** (1997) 221.

[12] H1 Collaboration, C. Adloff et al., *DESY* **99-010**, to appear in *Eur.Phys.J.*

[13] H1 Collaboration, C. Adloff et al., *Eur. Phys. J.* **C10** (1999) 373.

[14] L. Frankfurt, W. Koepf, M. Strikman, *Phys. Rev.* **D54** (1996), 319.
L. Frankfurt, W. Koepf, M. Strikman, *Phys. Rev.* **D57** (1998), 512.

[15] J. Collins, *Phys. Rev.* **D57** (1998) 3051.

[16] G. Ingelman, P. Schlein, *Phys. Lett.* **B152** (1985) 256.

[17] L. Alvero, J. Collins and J. Whitmore, *Phys. Rev.* **D59** (1999) 074022.

[18] H1 Collaboration, 'Diffractive dijet electroproduction at HERA', paper 157ae contributed to EPS99, Tampere, Finland, 1999

[19] J. Bartles, H. Lotter, M. Wüsthoff, *Phys. Lett.* **B379** (1996) 239.
J. Bartles, C. Ewerz, H. Lotter, M. Wüsthoff, *Phys. Lett.* **B386** (1996) 389.

[20] H1 Collaboration, 'Measurement of the production of D^* mesons in deep-inelastic diffractive interactions at HERA', Paper 157ag contributed to EPS99, Tampere, Finland, 1999.
P. Thompson, 'Open Charm Production in Inclusive and Diffractive Deep-Inelastic Scattering at HERA', Ph.D. thesis (University of Birmingham), 1999.

[21] H1 Collaboration, C. Adloff et al., Eur.Phys.J. **C6** (1999) 421.

[22] J. Bjorken, Phys. Rev. **D47** (1993) 101.
E. Gotsman, E. Levin, U. Maor, Phys. Lett. **B309** (1993) 199.
E. Gotsman, E. Levin, U. Maor, TAUP 2485-98, hep-ph/9804404.

[23] S. Abachi et al (D0 collaboration), Phys. Rev. Lett. 72 (1994) 2332; Phys. Rev. Lett. 76 (1996) 734; B. Abbott et al (D0 collaboration), Phys. Lett. B440 (1998) 189.

[24] F. Abe et al (CDF collaboration), Phys. Rev. Lett. 74 (1995) 855; Phys. Rev. Lett 80 (1998) 1156; Phys. Rev. Lett. 81 (1998) 5278.

[25] M. Derrick et al (ZEUS collaboration), Phys. Lett. B369 (1996) 55.

[26] J.R. Forshaw and P.J.Sutton, Eur.Phys.J. C1 (1998) 285.

[27] E.A.Kuraev, L.N.Lipatov and V.S.Fadin, Sov.Phys.JETP 45 (1977) 199.
Ya.Ya.Balitsky and L.N.Lipatov, Sov.J.Nucl.Phys 28 (1978) 822.
L.N.Lipatov, Sov.Phys.JETP 63 (1986) 904.

[28] A.H. Mueller and W.-K. Tang, Phys.Lett. B284, (1992) 123.

[29] B.E. Cox, J.R. Forshaw, L. Lönnblad, JHEP10(1999)023.

[30] H1 Collaboration, "Production of J/ψ Mesons with large $|t|$ at HERA", contribution to the International Europhysics Conference on High Energy Physics, Jerusalem, Israel (1997).

[31] J. Crittenden, "Recent Results from Decay-Angle Analyses of ρ^0 Photoproduction at High Momentum Transfer from ZEUS", contribution to the DIS99 Workshop, Zeuthen, Germany (1999) `hep-ex/9906005`.

[32] J. D. Bjorken, Phys. Rev. D471011993.

[33] E.Gotsman, E.Levin, U.Maor, Phys. Lett. B438 (1998) 229; Phys. Rev. D60 (1999)

[34] G. Oderda and G. Sterman, Phys. Rev. Lett. 81, 3591 (1998).

[35] S. D. Ellis and D. E. Soper, Phys. Rev. **D48** (1993) 3160.

[36] B. E. Cox, M. H. Seymour and A. C. Wyatt, in preparation.

[37] H1 Collaboration, DESY preprint DESY 00-037 and hep-ex/0003020.

[38] H1 Collaboration, 'Diffractive J/ψ Photoproduction', Paper 157o contributed to EPS99, Tampere, Finland, 1999.

[39] M.G.Ryskin, Z.Phys. C57 (1993) 89; and M.G.Ryskin et al., Z.Phys. C76 (1997) 231.

[40] A.D.Martin, M.G.Ryskin and T.Teubner, Phys.Lett. B454 (1999) 339.
L.Frankfurt,M.McDermott and M.Strikman, JHEP 02 (1999) 002.

[41] A.Donnachie and P.V.Landshoff, Phys.Lett. B348 (1995) 213.

[42] A.Donnachie and P.V.Landshoff, Phys.Lett. B437 (1998) 408.

[43] S.J.Brodsky et al., JETP Letters 70 (1999) 155.

[44] H1 Collaboration, C. Adloff et al., Nucl. Phys. B 538 (1999) 3.

[45] H1 Collaboration, C. Adloff et al., accepted by Eur. Phys. J. C.

[46] H1 Collaboration, C. Adloff et al., paper 157h, submitted to the International Europhysics Conference on High Energy Physics.

[47] H1 Collaboration, C. Adloff et al., *Phys. Lett.* **B467** (1999) 156.

[48] T. Sjöstrand and G. A. Schuler, Phys. Lett. **B376** (1996) 193;
M. Glück, E. Reya and M. Stratmann, Phys. Rev. **D54** (1996) 5515;
M. Drees and R. Godbole, Phys. Rev. **D50** (1994) 3124;
F. Borzumati and G. Schuler, Z. Phys. **C58** (1993) 139.

[49] H1 Collaboration, "Measurement of Di-Jet Cross-Sections at Low Q^2 and the Extraction of an Effective Parton Density for the Virtual Photon", DESY preprint 98-205 submitted to Eur. Phys. J. C.

[50] H1 Collaboration, C. Adloff et al., 29th International Conference on High Energy Physics ICHEP98, Vancouver, Canada, July 1998 No. 531

[51] P. Dixon, D. Kant and G. Thompson, Fragmentation Function Scaling Violations in the Breit Frame, submitted for the proceedings of the 3rd UK Phenomenology Workshop 20th-25th September 1998

[52] K.T. Donovan, D. Kant and G. Thompson, Rapidity Plateaux in the Breit Frame, submitted for the proceedings of the 3rd UK Phenomenology Workshop 20th-25th September 1998

[53] D. Kant, QCD Studies in the Breit Frame at HERA, Nucl. Phys. B (Proc. Suppl.) 71 (1999) 31-38.

[54] R.K. Griffiths, Ph.D thesis, University of London, 1998

[55] D. Graudenz, CERN TH/96-52, CERN TH/96-155 (hep-ph/9606460), CERN TH/96-187 (hep-ph/9610287)

[56] K.T. Donovan, Ph.D thesis, University of London, 1998.

[57] W. Ochs, Proceedings of the Ringberg Worshop "New Trends in HERA Physics", Tegernsee, Germany, 25-30 May 1997 hep/ph/9709248.

[58] "Fragmentation Functions and Rapidity Spectra in the Breit Fram D. Kant, *Nuclear Physics* **B 79** (Proc. Suppl.) (1999) 453.

[59] H1 Collaboration, Eur. Phys. J. C 12, 595-607 (2000).

[60] R.-D. Appuhn et al., The electronics of the H1 lead/scintillating-fibre calorimeters, *Nucl. Instr. and Meth.* **A426** (1999) 518.

[61] H1 Collaboration, "Proposal for an Upgrade of the H1 Forward Track Detector for HERA 2000", DESY PRC proposal **PRC 98-06**, 1998.

[62] H1 Collaboration, "A fast Track Trigger with High Resolution for H1" and "Addendum", DESY PRC Proposals **PRC 99-06** and **PRC 99-07**, 1999.

7 H1 Publications 3/98 to 3/00

The following have been published by the H1 Collaboration in the period March 1998 to March 2000.

1. "Photo-production of $\psi(2S)$ Mesons at HERA", DESY-97-228,submitted to Phys. Lett. B.
2. "Hadron Production in Diffractive Deep Inelastic Scattering", Phys. Lett. B428 (1998) 206-220
3. "Multiplicity Structure of Hadronic Final States in Diffractive Deep-Inelastic Scattering at HERA", Eur. Phys. J. C 5 (1998) 3, 439-452
4. "Observation of Events with an Isolated High Energy Lepton and Missing Transverse Momentum at HERA", Eur. Phys. J. C 5 (1998) 4, 575-584
5. "Differential (2+1) Jet Rates and Determination of α_s in Deep-Inelastic Scattering at HERA", Eur. Phys. J. C 5 (1998) 4, 625-639
6. "Di-Jet Event Rates in Deep-Inelastic Scattering at HERA", DESY-98-076 / submitted to Eur. Phys. J. C
7. "Multi-Jet Event Rates in Deep-Inelastic Scattering and Determination of the Strong Coupling Constant", DESY-98-087 / submitted to Eur. Phys. J. C
8. "Diffractive Dijet Production at HERA", DESY-98-092 / submitted to Eur. Phys. J. C
9. "Forward Jet and Particle Production at HERA", DESY-98-143 / submitted to Nucl. Phys. B
10. "Charged Particle Cross Sections in Photoproduction and Extraction of the Gluon Density in the Photon", DESY-98-148 / submitted to Eur. Phys. J. C
11. "Measurement of Leading Proton and Neutron Production in Deep Inelastic Scattering at HERA", DESY-98-169 / submitted to Eur. Phys. J. C
12. "Measurement of D^* Meson Cross Sections at HERA and Determination of the Gluon Density in the Proton", *Nucl.Phys.* **B545** (1999) 21.
13. "Measurement of Dijet Cross-Sections at Low Q^2 and the Extraction of an Effective Parton Density for the Virtual Photon", *DESY* **98-205**, to appear in *Eur. Phys. J.*
14. "Measurement of Internal Jet Structure in Di-jet Production in Deep Inelastic Scattering at HERA" *Nucl.Phys.* **B545** (1999) 3.
15. "Elastic Electroproduction of ρ^0 Mesons at HERA", *DESY* **99-010**, to appear in *Eur.Phys.J.*
16. "Charmonium Production in Deep Inelastic Scattering at HERA", *Eur. Phys. J.* **C10** (1999) 373.
17. "A Search for Leptoquark Bosons and Lepton Flavor Violation in Positron-Proton Collisions at HERA", *Eur. Phys. J.* **C11** (1999) 447.

18. "Measurements of Transverse Energy Flow in Deep-Inelastic Scattering at HERA" *DESY* **99-091**, accepted by *Eur. Phys. J.*

19. "Forward π^0-Meson Production at HERA", *Phys. Lett.* **B462** (1999) 440.

20. "Measurement of Neutral and Charged Current Cross-Sections in Positron-Proton Collisions at Large Momentum Transfer", *DESY* **99-107**, submitted to Eur Phys J.

21. "Measurement of Open Beauty Production at HERA", *Phys. Lett.* **B467** (1999) 156.

22. "Investigation of Power Corrections to Event Shape Variables measured in Deep-Inelastic Scattering" *DESY* **99-193**, submitted to *Eur. Phys. J.*

8 Theses: 3/98 to 3/00

All Ph. D theses which are concerned with *ep* physics at H1 and which have been submitted in the period March 1998 to March 2000 are listed below.

1. "Elastic J/ψ Photoproduction and the Detection and Trigerring of Muons al Low W using the H1 Detector", Kirstee Hewitt (Birmingham).

2. "Charged Particle Transverse Momentum Spectra in Positron Proton Collisions at the H1 Experiment", Theo Holtom (Liverpool).

3. "Rho prime Electroproduction at HERA", Stuart Cocks (Liverpool).

4. "Measurement of the Cross Section for the Elastic Photoproduction of the J/ψ Meson at HERA", M. Anderson (Manchester).

5. "Double Diffraction Dissociation at Large Momentum Transfer", B. Cox (Manchester).

6. "The First Measure of Relative Partonic Contributions in DIS at HERA using an Average Hadronic Charge", Robert K. Griffiths (QMW).

7. "Hadronic Fragmentation Studies in *ep* Scattering at HERA", Keith T. Donovan (QMW).

8. "A Measurement of Jet Cross Sections at Low Q^2 and an Interpretation of the results in terms of a Partonic Structure of the Virtual Photon", Mark Smith (Liverpool).

9. "Open Charm Production in Inclusive and Diffractive Deep-Inelastic Scattering at HERA", Paul Thompson (Birmingham).

10. "The Diffractive Production of J/ψ Vector Mesons with High Transverse Momenta at HERA", Duncan Brown (Manchester).

11. "High Transverse Momentum 2-Jet and 3-Jet Cross Section Measurements in Photoproduction", Paul Bate (Manchester).

9 H1 Conference Presentations: 3/98 to 3/00

Conference presentations (from March 1998) by members of the H1–UK groups which are concerned with all aspects of H1 physics and operation are listed below. They include "write-ups" of talks which were given before March 1998 but which were published since March 1998.

1. B. Cox, "Jets and Rapidity Gaps at HERA", in Proc. 3^{rd} LAFEX International School on High Energy Physics, Rio, February 1998.

2. B. Cox, "VDM Production at HERA", in Proc. 3^{rd} LAFEX International School on High Energy Physics, Rio, February 1998.

3. S. Maxfield, "Jets and the Hadronic Final State at HERA", in Proc. 12^{th} Rencontre de Physique de la Vallee D'Aoste, Aosta Valley, Italy, March 1998.

4. P. Newman,"Inclusive Diffraction and Leading Baryon Production at HERA", in Proc. 34^{th} Rencontres de Moriond, Les Arcs, France, March 1998.

5. T. Greenshaw, "Recent Results from H1", in Proc. 6^{th} International Workshop on Deep Inelastic Scattering and QCD, Brussels, April 1998.

6. B. Waugh, "Diffractive Final States", in Proc. 6th International Workshop on Deep Inelastic Scattering and QCD, Brussels, April 1998.

7. P. Thompson, "Heavy Vector Mesons at HERA", in Proc. 6th International Workshop on Deep Inelastic Scattering and QCD, Brussels, April 1998.

8. B. Cox, "Rapidity Gaps between Jets at HERA", in Proc. 6th International Workshop on Deep Inelastic Scattering and QCD, Brussels, April 1998.

9. A. Mehta, "Structure Functions at HERA", in Proc. 6th International Workshop on Deep Inelastic Scattering and QCD, Brussels, April 1998.

10. E. Rizvi, "QCD Analysis of Structure Funcions", in Proc. 6th International Workshop on Deep Inelastic Scattering and QCD, Brussels, April 1998.

11. B. Cox, "Isolating the Hard Pomeron at HERA", talk given at the Institute of Physics Conference, Manchester, April 1998.

12. K. Donovan, "Charged Particle Spectra in the Breit Frame at HERA", talk given at the Institute of Physics Conference, Manchester, April 1998.

13. M. Smith, "Low Q^2 Jet Production at HERA", talk given at the Institute of Physics Conference, Manchester, April 1998.

14. P. Thompson, "D^* Production in Diffractive DIS with the H1 Detector", talk given at the Institute of Physics Conference, Manchester, April 1998.

15. J. Dainton, "The Future of ep Physics at HERA", talk given at "Aspects of Deep Inelastic Scattering", Berlin-Zeuthen, June 1998.

16. T. Greenshaw, "QCD at HERA", invited contribution presented at the High Energy Physics Forum, Abingdon, June 1998.

17. D. Milstead, “Forward Jet and Particle Production at HERA”, talk given at “Aspects of Deep Inelastic Scattering”, Berlin-Zeuthen, June 1998.

18. D. Kant, “Fragmentation Functions and Event Shapes in the Breit Frame”, talk given at “Aspects of Deep Inelastic Scattering”, Berlin-Zeuthen, June 1998.

19. J. Phillips, “H1 Physics Results”, talk given to Extended Scientific Council, DESY, Hamburg, June, 1998.

20. C. Hilton, “Heavy Vector Meson Production at HERA”, in Proc. 3^{rd} International Conference on Hyperons, Charm and Beauty, Geneva, July, 1998.

21. D. Milstead, “Forward Jet and Particle Production at HERA”, in Proc. 29^{th} International Conference on High Energy Physics, Vancouver, July 1998.

22. D. Milstead, “QCD in the Hadronic Final State at HERA”, in Proc. 28^{th} International Symposium on Multi-particle Dynamics, Delphi, Greece, September 1998.

23. P. Newman, “Diffractive Phenomena in ep Physics”, in Proc. International Conference on Hadron Structure, Stara Lesna, Slovakia, September 1998.

24. B. Cox, “Rapidity Gaps between Jets”, in Proc. 4th Workshop on Small-x and Diffractive Physics, Fermilab, US, September 1998.

25. B. Cox, “Experimental Results in Small x Physics and Diffraction”, talk given at the Workshop on HERA Physics, Durham, September 1998, to appear in J. Phys. G.

26. D. Kant, “Can we see the Signature of LPHD Resolvable Gluons at HERA?”, talk given at the Workshop on HERA Physics, Durham, September 1998, to appear in J. Phys. G.

27. P. Dixon, “Scaling Violation of ep DIS Fragmentation Functions at HERA”, talk given at the Workshop on HERA Physics, Durham, September 1998, to appear in J. Phys. G.

28. G. Thompson, “Jets and Fragmentation”, summary talk given at the Workshop on HERA Physics, Durham, September 1998, to appear in J. Phys. G.

29. E. Rizvi, “Neutral and Charged Current DIS at high Q^2”, 13th Topical Conference on Hadron Collider Physics (Hadron13), Mumbai, India, January 1999.

30. A. Mehta, “The Outlook for HERA”, 13th Topical Conference on Hadron Collider Physics (Hadron13), Mumbai, India, January 1999.

31. J. Dainton, “The Structure of Hadronic Physics”, Max Born Lecture, Annual meeting of the German Physical Society, Heidelberg, Germany, March 1999.

32. T. McMahon, “Studies of real and virtual photon structure at HERA”, 34th Rencontres de Moriond: QCD and Hadronic Interactions, Les Arcs, France, March 1999.

33. B. Cox, “High t diffraction at HERA”, 7th International Workshop on Deep-Inelastic Scattering and QCD (DIS99), Zeuthen, Germany, April 1999.

34. P. Newman, “H1 Measurements of Open b Production”, 7th International Workshop on Deep-Inelastic Scattering and QCD (DIS99), Zeuthen, Germany, April 1999.

35. D. Kant, "Fragmentation functions and rapidity spectra in the Breit frame at H1", 7th International Workshop on Deep-Inelastic Scattering and QCD (DIS99), Zeuthen, Germany, April 1999.

36. B. Cox, "High t Diffraction", Institute of Physics Conference, Salford, April 1999.

37. B. Waugh, "Elastic/Diffractive Vector Meson Production in Photoproduction", International Conference on the Structure and Interactions of the Photon (PHOTON99), Freiburg, Germany, May 1999.

38. P. Thompson, "Production of D^* mesons in deep-inelastic diffractive interactions at HERA", International Conference on the Structure and Interactions of the Photon (PHOTON99), Freiburg, Germany, May 1999.

39. T. Greenshaw, "Forward Jet and Hadron Production at Low x and Q^2", Ringberg HERA Phenomenology Workshop, Bavaria, Germany, May 1999.

40. J. Dainton, "Low x Physics", Frontiers of Matter (Rencontres de Blois), Gif-sur-Yvette, France, July 1999.

41. P. Newman, "Introductory Talk on Low-x and Diffractive Physics", UK Phenomenology Workshop on Collider Physics, Durham, UK, September 1999.

42. B. Cox, "Summary Talk on Low-x and Diffractive Physics", UK Phenomenology Workshop on Collider Physics, Durham, UK, September 1999.

43. J. Dainton, "Electron-Proton Physics at HERA - Beyond the Beginning", International Workshop on Symmetry and Spin (PRAHA-SPIN '99), Prague, Czech Republic, September 1999.

44. J. Dainton, "Low x Physics", International Workshop on Symmetry and Spin (PRAHA-SPIN '99), Prague, Czech Republic, September 1999.

45. D. Milstead, "Fragmentation and Power Corrections", XXIX International Symposium on Multiparticle Dynamics (ISMD99), Rhode Island, USA, Aug 1999.

46. A. Mehta, "Latest Results from HERA", 7th International Symposium on Particles, Strings and Cosmology (PASCOS99), Lake Tahoe, USA, December 1999.

10 H1 Conference Submissions: 3/98 to 3/00

The following papers were submitted by the H1 collaboration to the 29^{th} International Conference on High Energy Physics, Vancouver, July, 1998.

1. Abstract 520: "Measurement of Dijet Cross Sections in Deep Inelastic Scattering at HERA"

2. Abstract 523: "Di-jet Rates in Deep Inelastic Scattering at HERA"

3. Abstract 527: "Multi-Jet Event Rates in Deep-Inelastic Scattering and Determination of the Strong Coupling Constant"

4. Abstract 528: "Differential (2+1) Jet Rates and Determination of α_s in Deep-Inelastic Scattering at HERA"
5. Abstract 529: "Forward Jet and Particle Production at HERA"
6. Abstract 530: "Measurement of Event Shape Variables in Deep Inelastic *ep* Scattering at HERA"
7. Abstract 531: "Evolution of ep Fragmentation and Multiplicity Distributions in the Breit Frame"
8. Abstract 532: "Measurement of Internal Jet Structure in Dijet Production in Deep Inelastic Scattering and Photoproduction"
9. Abstract 533: "Measurement of Inclusive Cross Sections for Neutral and Charged Current Interactions at High-Q^2"
10. Abstract 534: "Precision Measurement of the Inclusive Deep Inelastic ep Scattering Cross Section at Low Q^2 at HERA"
11. Abstract 535: "Low Q^2 – Intermediate x Structure Function Measurement at HERA"
12. Abstract 544: "Measurement of Di-jet Cross-sections in Low Q^2 Deep-Inelastic Scattering Processes at HERA and the Extraction of an Effective Parton Density of the Virtual Photon"
13. Abstract 549: "Dijet Cross Sections in Photoproduction and Determination of the Gluon Density in the Photon"
14. Abstract 551: "High P_t Charged Particle Cross Section in Photoproduction and Extraction of the Gluon Density in the Photon"
15. Abstract 553: "Transverse Energy Production in Deep-Inelastic Scattering"
16. Abstract 556: "Measurement of the Baryon-Antibaryon Asymmetry in Photoproduction at HERA"
17. Abstract 576: "Inclusive Photoproduction of π^0 Mesons in the Photon Hemisphere at HERA"
18. Abstract 578: "Observation of Events with an Isolated High Energy Lepton and Missing Transverse Momentum at HERA"
19. Abstract 579: " Search for Leptoquark Bosons in DIS at High Q^2 at HERA"
20. Abstract 580: "A Search for Squarks of R-Parity Violating SUSY at HERA"
21. Abstract 581: "Search for Excited Fermions at HERA"
22. Abstract 584: "A Search for Contact Interactions in Neutral Current Scattering at HERA"
23. Abstract 585: "Antideuteron Production at HERA and Search for Heavy Stable Charged Particles"

The following papers were submitted by the H1 collaboration to both the International Europhysics Conference on High Energy Physics (EPS 99), Tampere, Finland and the International Symposium on Lepton and Photon Interactions at High Energies (LP99), Stanford, USA, unless other indicated.

1. EPS99 Abstract 157s, “Search for events with an isolated high energy lepton and missing transverse momentum at HERA”
2. EPS99 Abstract 157u, “Test of the Standard Model in high E_T jet production at HERA”
3. EPS99 Abstract 157c, “A Search for Leptoquark Bosons and Lepton Flavor Violation in Positron-Proton Collisions at HERA”
4. EPS99 Abstract 157f, “A Search for Contact Interactions in Neutral Current Scattering at HERA”
5. EPS99 Abstract 157ai, “Measurement of Neutral and Charged Current Cross-Sections in Positron-Proton Collisions at Large Momentum Transfer at HERA”
6. EPS99 Abstract 157b, “Measurement of the Neutral and Charged Current Cross Sections in Electron-Proton Collisions at High Q^2 at HERA”
7. EPS99 Abstract 157p, “Measurement of D^* Meson Cross Sections at HERA and Determination of the Gluon Density in the Proton using NLO QCD”
8. EPS99 Abstract 157r, “Measurement of Dijet Cross-Sections at Low Q^2 in ep Collisions and the Extraction of an Effective Parton Density for the Virtual Photon”
9. EPS99 Abstract 157j, “Study of the photon remnant in resolved photoproduction and low Q^2 processes at HERA”
10. EPS99 Abstract 157ad, “Dijet Cross Sections in Photoproduction and Determination of the Gluon Density in the Photon”
11. EPS99 Abstract 157g, “Test of QCD Dynamics at Small Parton Momenta x at HERA”
12. EPS99 Abstract 157, “Determination of the Strong Coupling Constant from Inclusive Jet Cross Sections”
13. EPS99 Abstract 157, “Measurement of Differential Jet Production in Deep-Inelastic Scattering at High Q^2 at HERA”
14. EPS99 Abstract 157 “Study of Three-Jet Production in Deep-Inelastic Positron Proton Collisions at HERA”
15. EPS99 Abstract 157x, “Measurement of Internal Jet Structure in Dijet Production in Deep-Inelastic Scattering at HERA”
16. EPS99 Abstract 157ae, “Diffractive dijet electroproduction at HERA”
17. EPS99 Abstract 157m, “Measurement of Leading Proton and Neutron Production in Deep Inelastic Scattering at HERA”
18. EPS99 Abstract 157ag, “Measurement of the production of D^* mesons in deep-inelastic diffractive interactions at HERA”

19. EPS99 Abstract 157o, "Charmonium Production in Deep Inelastic Scattering at HERA"

20. EPS99 Abstract 157aj, "Inelastic Photoproduction of J/ψ and $\psi(2S)$"

21. EPS99 Abstract 157n, "Proton Dissociative and Elastic Electroproduction of ρ^0 Mesons at HERA"

22. EPS99 Abstract 157k, "A study of event shape variables in deep-inelastic ep scattering at HERA"

23. EPS99 Abstract 157l, "Transverse energy flow in deep-inelastic ep Scattering at HERA"

24. EPS99 Abstract 157h, "A study of inclusive identified charged particle production in deep-inelastic scattering at HERA"

25. LP99 only, "W Production in $e^{\pm}$ collisions at HERA"

11 H1–UK Manpower: 3/98 to 3/00

Manpower which has contributed to the on–going H1 physics programme is listed below for each H1–UK institute.

1. **University of Birmingham**
   Y. Coppens, J. Dowell, P. Faulkner, Y. Fleming J. Garvey, C. Goodwin, I. Kenyon, D. Lamb, P. Newman, E. Rizvi, P. Sutton, P. Thompson, L. West.

2. **University of Lancaster**
   R. C. W. Henderson, T. Sloan, G. R. White.

3. **University of Liverpool**
   A. Burrage, S. Cocks, C. Cormack, J.B. Dainton, E. Gabathuler, T. Greenshaw, B. Heinemann, T. Holtom, M. Jones, J. Kennedy, P. Laycock, S.J. Maxfield, T. McMahon, A. Mehta, D. Milstead, J.M. Morton, G.D. Patel, J.P. Phillips.

4. **University of Manchester**
   M. Anderson, P. Bate, P. Biddulph, D.P. Brown, B. Cox, J.M. Foster, C.D. Hilton, M. Ibbotson, S. Koyla, N. Malden, R. Marshall, D. Mercer, K. Stephens, B. Waugh.

5. **Queen Mary and Westfield College, University of London**
   K.T. Donovan, E.F. Eisenhandler, R.K. Griffiths, D. Kant, A. Kirby, M.J.P.I. Landon, B. Morgan, G. Thompson.

6. **CLRC Rutherford Appleton Laboratory**
   D. Clarke, J.A. Coughlan, W.J. Haynes, D.L. Hill, J.V. Morris, T.C. Nicholls, D.P.C. Sankey.

12 H1–UK Physicists with General Responsibilities

The following have held positions of central responsibility for H1 during the period March 1998 to March 2000.

12.1 University of Birmingham

1. P. Newman: co–convenor – H1 Physics Working Group "Diffractive Phenomena" (until 01/99).

2. P. Thompson: H1TRIG librarian.

3. E. Rizvi: co–convenor H1 Technical Working Group "Fitting Techniques".

4. L. West: H1 PHAN coordinator (until 10/98).

12.2 University of Lancaster

1. S. Burke: H1 FTD Software Convenor, H1 Reconstruction Coordinator (until 12/98).

12.3 University of Liverpool

1. J.B. Dainton: Spokesman (until 08/99).

2. T. Greenshaw: co–convenor – H1 Physics Working Group "Flow and Spectra Group Phenomena", Project Co-ordinator for the $8m$ Tagger.

3. S. Maxfield: co–convenor – H1 Physics Working Group "Jets"

4. A. Mehta: co–convenor – H1 Physics Working Group "High P_T and Q^2".

5. D. Milstead: co-convenor – H1 Physics Working Group "Flow and Spectra".

6. J.P. Phillips: co–convenor – H1 Technical Working Group "Energy Scale and Calibration".

12.4 University of Manchester

1. P. Biddulph: H1 Technical Coordinator (until 08/98).

2. B. Cox: H1-UK Public Understanding of Science (PUS) Coordinator.

3. C. Hilton: co–convenor H1 Physics Working Group "Heavy Flavour" (until 12/98).

4. B. Waugh: H1 Forward Muon Detector Coordinator.

12.5 Rutherford Appleton Laboratory

1. D. Clarke: H1 Forward Track Detector Coordinator.

2. W.J. Haynes: H1 Central DAQ Coordinator (until 08/99).

3. D. Sankey: Fast Track Trigger UK Coordinator.

In addition to the above, UK physicists have taken their share of responsibilities as H1 Run Co-ordinators during data taking. H1–UK physicists are regularly asked to be collaboration referees for putative H1 publications concerned with the work of others. During the period of this report, P. Biddulph (*ex.officio*), J. Dainton (*ex.officio*), T. Sloan and T. Greenshaw have served as members of the H1 Executive Committee.